

Systemic risk in markets with multiple central counterparties

Luitgard Anna Maria Veraart¹  | Iñaki Aldasoro²

¹Department of Mathematics, London School of Economics and Political Science, London, UK

²Bank for International Settlements, Basel, Switzerland

Correspondence

Luitgard Anna Maria Veraart,
Department of Mathematics, London School of Economics and Political Science, Houghton Street, London WC2A 2AE, UK.

Email: L.Veraart@lse.ac.uk

Funding information

Bank for International Settlements, Grant/Award Number: BIS Research Fellowship

Abstract

We provide a framework for modeling risk and quantifying payment shortfalls in cleared markets with multiple central counterparties (CCPs). Building on the stylized fact that clearing membership is shared among CCPs, we develop a modeling framework that captures the interconnectedness of CCPs and clearing members. We illustrate stress transmission mechanisms using simple examples as well as empirical evidence based on calibrated data. Furthermore, we show how stress mitigation tools such as variation margin gains haircutting by one CCP can have spillover effects on other CCPs. The framework can be used to enhance CCP stress-testing, which currently relies on the “Cover 2” standard requiring CCPs to be able to withstand the default of their two largest clearing members. We show that who these two clearing members are can be significantly affected if one considers higher-order effects arising from interconnectedness through shared clearing membership. Looking at the full network of CCPs and shared clearing members is, therefore, important from a financial stability perspective.

This is an open access article under the terms of the [Creative Commons Attribution](https://creativecommons.org/licenses/by/4.0/) License, which permits use, distribution and reproduction in any medium, provided the original work is properly cited.

© 2024 The Author(s). *Mathematical Finance* published by Wiley Periodicals LLC.

KEYWORDS

central counterparties, contagion, Cover 2, stress testing, systemic risk

JEL CLASSIFICATION

C60, C62, G18, G21, G23

1 | INTRODUCTION

Central clearing has become a key feature of global derivatives markets in the aftermath of the Global Financial Crisis. The mandates to centrally clear derivatives have significantly altered the shape of financial networks—in centrally cleared markets a central counterparty (CCP) sits at the center, becoming the buyer to every seller and the seller to every buyer. Much of the academic and policy effort in understanding and managing risks in centrally cleared markets has been on the CCPs themselves and their ability to withstand a severe shock.¹ In theory, there are efficiency gains arising from having a single CCP (Duffie & Zhu, 2011). In practice, however, derivatives clearing is characterized not by a single CCP, but by a small set of CCPs. Importantly, linking these CCPs is a limited number of large banks representing the joint clearing membership that together account for the lion's share of clearing volumes.²

In this paper, we analyze the role of joint clearing membership at multiple CCPs for stress transmission and financial stability. Joint clearing membership affects the structure of interconnections in financial networks, connecting CCPs via their shared clearing members and connecting the latter via CCPs. As such, it can affect risk transmission (see, e.g., Faruqui et al., 2018 for a discussion of the economic mechanisms characterizing the nexus between CCPs and clearing members). In this context, the default management mechanism of CCPs plays a central role.³ This is usually described in terms of the “default waterfall,” which specifies the order of loss absorption for the resources available to CCPs (see, e.g., Duffie, 2014).

We show how joint clearing membership can affect several layers of the default waterfall. The exact structure of a waterfall varies between CCPs, but as outlined in Gregory (2014), it can be split into losses paid by defaulters and by survivors. In particular, initial losses are paid for by

¹ See Menkveld and Vuillemeij (2021) for a recent literature survey. A large part of the literature on central clearing focuses on counterparty credit risk and netting efficiency. Duffie and Zhu (2011) show that clearing different products in separate CCPs decreases netting efficiency and increases counterparty credit exposure, compared to clearing all products in one CCP. Despite the theoretical advantages, central clearing today is done by a group of CCPs and not just a single CCP. Cont and Kokholm (2014) consider a generalization of the Duffie and Zhu (2011) framework and show that some of the conclusions depend on distributional assumptions on exposures. Garratt and Zimmerman (2015) generalize this framework further by considering more general network structures (e.g., scale-free networks).

² BCBS-CPMI-FSB-IOSCO (2018) show that, empirically, central clearing is characterized by a strong concentration around clearing members. These tend to be the largest global dealer banks that have long dominated derivatives trading. The central role of these banks implies that they tend to be connected to more than one CCP, as they facilitate trading across both markets and jurisdictions. Huang (2019) provides a theoretical model of competition between CCPs, whereas Demange and Piquard (2021) provide empirical evidence of competition between CCPs in Europe.

³ While CCP defaults are very rare events, they are not without historical precedent (Bignon & Vuillemeij, 2020; Faruqui et al., 2018). Furthermore, recent empirical evidence based on European repo market data suggests the potential failure of a CCP is perceived as a real possibility by market participants and is priced into repo rates (Boissel et al., 2017).

the defaulting clearing members (in the form of initial margins (IMs) and their default fund contributions) and higher losses are paid for by the CCP (skin-in-the-game) and surviving clearing members (via their default fund contributions and potentially additional contributions). We show that joint clearing membership affects both parts of the default waterfall, that is, how the defaulters pay and how the survivors pay, giving rise to different contagion channels.

We consider two contagion channels associated with the default waterfall. The first is the fire-sale channel of IMs. IMs, typically in the form of collateral, serve as the first line of defense in the waterfall to cover losses associated with individual positions cleared via CCPs. A simultaneous default at more than one CCP by a joint clearing member can lead to losses larger than those covered by IMs at all the CCPs where the member clears—a situation which is only worsened if collateral is illiquid.⁴ The second channel we consider is associated with one of the last layers of the default waterfall: VM gains haircutting (VMGH).⁵ If a stressed CCP uses VMGH, then all clearing members who owe variation margin (VM) to this CCP are required to make full payments, but the CCP itself only pays out a fraction of the VM it owes. We show that one CCP's VMGH can transmit losses to another CCP via their joint clearing members. In the extreme, a clearing member could cause the default of an unrelated CCP if the CCP where it clears employs VMGH.

Finally, we show how illiquid collateral and VMGH interact, potentially leading to even larger losses, notably when the CCP-bank nexus consists of cycles (i.e., when CCPs are connected to each other via joint clearing members).⁶

To illustrate these channels, we build a network model where clearing members are connected to multiple CCPs through derivatives market obligations. The trigger for contagion is an exogenous change in market conditions giving rise to VMs between clearing members and CCPs. As VMs come due, counterparties attempt to meet them. If they cannot, then they are put on “technical default” and IMs and default fund contributions will be used. But if the collateral underpinning IMs is illiquid, the realized equilibrium price will likely be smaller than originally anticipated—further fueling shock transmission. If payment obligations cannot be met, clearing members effectively default, whereas CCPs can rely on VMGH, which in turn may curtail effective payments to other clearing members and further contribute to contagion. Along the way, at each stage, stress can be transmitted across CCPs and clearing members due to the shared membership across CCPs. The model builds on the literature on systemic risk in financial networks and is particularly related to approaches that consider CCPs or the presence of collateral. Concretely, we build on Ghamami et al. (2022), who derive a modeling framework for clearing payments in collateralized networks (without a CCP) based on the seminal contribution by Eisenberg and Noe (2001). We adapt this framework to markets with multiple CCPs, allow for a more detailed default

⁴ Glasserman et al. (2015), who refer to this mechanism as “hidden illiquidity,” show that convex margin requirements incentivize clearing members to split their positions among several CCPs. They analyze the existence and characteristics of equilibria of margin schedules, such that CCPs collect sufficient margins in the presence of optimizing clearing members. However, they do not model the contagion mechanism itself that arises from illiquid collateral, which is what we study here. Throughout the paper, we use the short-hand of “illiquid margins” to refer to the illiquidity of the collateral with which margins are met.

⁵ We cover details of the default waterfall below. ISDA (2013) advocates the use of variation margin gains haircutting for failing CCPs: “For Default Losses, this paper advocates Variation Margin Gains Haircutting (‘VMGH’) as a robust recovery and continuity mechanism which will operate as part of the default waterfall following the exhaustion of all other layers of the default waterfall.”

⁶ Throughout, the default of a clearing member (given by an inability to meet payments due on derivatives) is invariably at the root of a CCP's default.

mechanism of CCPs, and include frictions such as default costs (in the spirit of Rogers & Veraart, 2013) and the possibility of VMGH by CCPs.⁷

The modeling framework we present works for general network structures and does not make any assumptions about the magnitudes of different layers of the default waterfall. A growing literature considers design aspects of central clearing. For example, Amini et al. (2015) study the problem of designing central clearing such that it reduces systemic risk and is consistent with the preferences of those using it. Biais et al. (2016) study the optimal design for central clearing and margin calls to increase resilience in derivatives markets. Lopez et al. (2017) propose a methodology for estimating margin requirements that accounts for interdependencies of market participants. Wang et al. (2022) propose a normative analysis on the design of collateral requirements for central clearing. They consider both IMs and default funds in their analysis. Huang (2019) consider the incentive problem of thin skin-in-the-game of CCPs. In contrast to these approaches, we take the design as given and analyze the outcome for a given design. There is considerable flexibility, however, in the specific design that can be considered in our analysis.

We use three stylized examples to illustrate how contagion through joint clearing membership and multiple CCPs operates in the model. The first and most simple has a clearing member jointly clearing in two CCPs and two additional clearing members clearing only at each of the two CCPs. The default of the joint clearing member can cause large losses to both CCPs, in the extreme potentially leading to their default if the collateral posted by the defaulting member is illiquid.⁸ The second example has a similar structure, but the default is of a clearing member that only clears at one CCP. This example helps to illustrate the possibility that the default of a clearing member can adversely affect a CCP in which the member *does not* clear. The third example involves a cycle where two clearing members jointly clear at two CCPs, and it helps to illustrate how the interaction of illiquid collateral and VMGH can help propagate distress and default in the network. Our analysis extends earlier work on the nexus between CCPs and clearing members (as analyzed for example in Faruqui et al., 2018) by providing a quantitative model to measure the magnitude of losses arising from the feedback loops between these agents.

Beyond these stylized examples, we provide empirical evidence of CCP-clearing member interconnectedness by analyzing public data on interest rate and credit default swaps (IRS and CDS, respectively). We calibrate our model based on data on clearing membership, notional amounts cleared (for both members and CCPs), default funds, skin-in-the-game, and aggregate IMs, as well as estimates of the network of payments obligations and liquidity buffers. We use this to quantify the shortfall in payments when accounting for higher-order effects and the different contagion channels discussed above. Our analysis helps to illustrate that the mechanisms captured by the model could be of relevance when calibrated to real-world data. That said, our exercises are meant as illustrative of the mechanisms we model, rather than a real-world stress test—in other words, we cannot quantify the likelihood of any scenario leading to an actual CCP default.

Our results carry important policy implications, in particular regarding CCP stress-testing.⁹ At the heart of the current practice is the Cover-2 standard, which, generally speaking, seeks to

⁷ Our work also relates to Paddrik et al. (2020) and Paddrik and Young (2021), who model payment shortfalls in centrally cleared markets with a single CCP. In contrast, we consider markets with multiple CCPs, model in more detail the CCP default waterfall and include additional frictions such as default costs and different magnitudes of variation margin gains haircutting into the modeling framework.

⁸ In both the model and the simulations that follow, a CCP can default if it is not able to meet its payment obligations to clearing members (after recourse to available elements from the default waterfall).

⁹ See CPMI-IOSCO (2018) for a general framework of supervisory stress testing of CCPs. For details on current market practice for stress testing CCPs in the European Union, we refer to ESMA (2020).

identify the two groups of clearing members that would lead to the largest shortfall of prefunded resources for a given CCP or alternatively across all CCPs.¹⁰ Paddrik and Young (2021) argue that the Cover-2 standard can underestimate the vulnerability of the system because it does not consider network effects. They provide empirical evidence for such network effects in a single-CCP market, allowing for VMGH. By considering only one CCP, however, their analysis abstracts from the effects of joint clearing members in loss transmission between several CCPs—what we analyze here. In our simulations, the total loss can increase by a factor of around four when considering network effects with multiple CCPs, shared clearing members and the contagion channels discussed above.

We argue that who the top two clearing members are (that cause the highest losses) will significantly depend on the contagion mechanisms included in the modeling framework. In particular, we show that the ranking of institutions according to first-order losses can differ notably from that obtained when considering higher-order losses that account for shared clearing membership.¹¹ From a financial stability perspective, it is thus important to take into account the network of joint clearing membership across multiple CCPs.

The main contributions of our paper are two-fold. First, we develop a framework to quantify payment shortfalls in centrally cleared markets with multiple CCPs and identify different roles of joint clearing members for loss transmission. Furthermore, we show how stress mitigation mechanisms such as VMGH by one CCP can have spill-over effects to other CCPs. Second, we discuss policy implications for stress testing CCPs focusing in particular on the Cover-2 standard. We show that who the two top clearing members are varies significantly depending on whether one accounts for contagion effects via joint clearing membership and defaults at multiple CCPs. Our analysis, therefore, can serve as a tool to select stress scenarios in markets with multiple CCPs.

The rest of the paper is structured as follows. Section 2 presents the modeling framework and its various variants. Section 3 provides simple stylized examples to illustrate how contagion unfolds in the model. Section 4 presents evidence of CCP interconnectedness through joint clearing membership in interest rate and credit default swap markets. Section 5 shows how our modeling framework can be used for CCP stress testing and discusses policy implications. Finally, Section 6 concludes.

2 | MODELING CONTAGION IN MARKETS WITH MULTIPLE CCPS

We develop a model for a clearing equilibrium in derivatives markets when VMs become due. Our model is a generalized version of the model proposed by Ghamami et al. (2022), which itself builds on the clearing framework developed by Eisenberg and Noe (2001). We adapt this to markets with multiple CCPs and introduce additional frictions to account for risk-mitigation tools available to CCPs, in particular VMGH.

Ghamami et al. (2022) propose a clearing mechanism for collateralized markets that proceeds in two rounds. The first round determines who defaults, as well as the initial payments made between counterparties. In the second round, collateral (IM) that was not used is returned to the nodes that originally set it aside and is used to make additional payments if those made in the first

¹⁰ See Section 5 for details on the two different types of applications of the Cover-2 standard.

¹¹ Cont (2017) highlights the importance of addressing liquidity risk in stress tests of CCPs rather than focusing only on counterparty credit risk and insolvency risk. Indeed, more recent stress tests, for example, ESMA (2020) explicitly consider liquidity risk in their stress test. Our analysis focuses on liquidity stress testing as well.

round fell short of obligations. We will generalize the first round of clearing to allow for market frictions (such as exogenous default costs) or different magnitudes of VMGH by CCPs, and use the second round of clearing without any modifications.¹²

We consider a financial market consisting of $n_M \in \mathbb{N}$ clearing members, with indices in $\mathcal{M} = \{1, \dots, n_M\}$ and $n_C \in \mathbb{N}$ CCPs with indices in $\mathcal{C} = \{n_M + 1, \dots, n_M + n_C\}$. We write $\mathcal{N} = \mathcal{M} \cup \mathcal{C}$ and set $N = n_M + n_C$. We assume that every clearing member clears their trades with at least one of the CCPs. Clearing members can have trading relationships with more than one CCP and indeed this can be observed in practice, as we will discuss in Section 4.

We assume that clearing members and CCPs are connected through a network of obligations arising from derivative positions.¹³ For example, these could represent a network of obligations arising from CDS written on a specific reference entity. Then, if the reference entity defaults, payments become due from the protection seller to the protection buyer in the CDS contract. But even if no default occurs, changes to market conditions can trigger payment obligations between the counterparties in the form of VM payments. In the following, we focus on networks of VM payment obligations, as, for example, in Paddrik et al. (2020) who consider such a setting in a market with one CCP.¹⁴

2.1 | First round of clearing and assessment of defaults

We assume that due to changes in market conditions, VMs become due. We denote by $\bar{p}^{\text{R1}} \in [0, \infty)^{N \times N}$ the VM obligations matrix, with element \bar{p}_{ij}^{R1} , where $i, j \in \mathcal{N}$, capturing the *VM payment obligation* from i to j . Since VMs are usually bilaterally netted, we assume that for all $i, j \in \mathcal{N}$ with $i \neq j$ at most one of p_{ij} and p_{ji} is strictly positive and $p_{ii} = 0$ for all $i \in \mathcal{N}$. Furthermore,

$$\bar{p}_i^{\text{R1}} = \sum_{j=1}^N \bar{p}_{ij}^{\text{R1}}$$

denotes the *total variation payment obligation* of firm $i \in \mathcal{N}$.

There are a number of resources available to the nodes in the system to meet payment obligations. For one, as part of the contractual arrangement that gives rise to potential payment obligations, counterparties post IM. We denote by $m_{ki} \geq 0$ the number of shares of the asset used as IM posted by k to i , where $k, i \in \mathcal{N}$, $k \neq i$ and $m_{ii} = 0$ for all $i \in \mathcal{N}$. As in Ghamami et al. (2022), we assume that all margin accounts are held in the same (potentially) illiquid asset. An important difference between CCPs and clearing members is that the latter are required to provide

¹² As our setting is similar to that in Ghamami et al. (2022), we try to use the same notation whenever possible, with adjustments to allow for the existence of CCPs.

¹³ We take this network as given and do not investigate further the mechanism that led to this particular network. In addition to clearing trades, CCPs often offer other services as well that could potentially influence the resulting network structure. For example, some offer portfolio compression, which is a post-trade mechanism in which positions that are economically redundant are eliminated, see Domanski et al. (2015), Schrimpf (2015), and Gregory (2014, Subsection 8.2.3) for further details. It is, for example, offered by LCH's SwapClear service (<https://www.lch.com/services/swapclear/enhancements>). For further details on the mechanisms of portfolio compression, we refer to O'Kane (2017) and D'Errico and Roukny (2021). Possible implications for systemic risk have been analyzed in Veraart (2022), and Amini and Feinstein (2023) have looked into portfolio compression focussing on an optimal market design.

¹⁴ It would be possible to explicitly model how the original obligations network can be mapped into a network of variation margin payments as in Veraart (2022), but for the purpose of our analysis, this is not strictly necessary.

IMs to the CCP at which they clear, whereas CCPs do not provide IMs to their clearing members (Ghamami et al., 2022, Appendix B). Hence, in our setting with multiple CCPs, we have $m_{ki} = 0$ for all $k \in C$ and for all $i \in \mathcal{N}$. Furthermore, clearing members also have liquidity buffers to deal with fluctuations in payment obligations and receipts (e.g., cash). We assume that $b^M \in [0, \infty)^{n_M}$ is the vector capturing such liquidity buffers, that is, each clearing member $i \in \{1, \dots, n_M\}$ has a liquidity buffer $b_i^M \geq 0$.

We account for the special structure of CCPs' liquidity buffers. As discussed above, a key feature of CCPs' risk management is the so-called default waterfall, which sets out the hierarchy and sequence of resources that CCPs can draw from to meet payment obligations arising from the default of one or more clearing members.

We explicitly model two prefunded resources that form part of the default waterfall of a CCP (in addition to the IMs), namely the default fund and the skin-in-the-game. The default fund refers to the contribution of clearing members to the financial resources of the CCP, whereas the skin-in-the-game refers to the (usually very thin) CCP's equity.¹⁵ This part of our model is a slight generalization of the model by Paddrik et al. (2020), who—in addition to modeling contagion in a single-CCP setting—consider only the default fund as a liquidity buffer. We denote by $\delta \in [0, \infty)^{n_C}$ the vector of CCPs' default funds, that is, δ_j is the default fund of CCP j . In particular,

$$\delta^T = \mathbf{1}_{n_M}^T \tilde{\delta},$$

where $\mathbf{1}_{n_M}$ is the n_M -dimensional unit vector and $\tilde{\delta} \in [0, \infty)^{n_M \times n_C}$ is the matrix with element $\tilde{\delta}_{ij}$ representing the default fund contribution of member i to CCP j .

We denote by $\sigma \in [0, \infty)^{n_C}$ the skin-in-the-game vector, that is, σ_j is the skin-in-the-game of CCP j . We then define a vector $b \in [0, \infty)^N$ as follows:

$$b_i = \begin{cases} b_i^M, & \text{if } i \in \mathcal{M}, \\ \delta_i + \sigma_i, & \text{if } i \in C. \end{cases}$$

Hence, b represents additional resources that are in principle available to cover payment shortfalls that are not covered by IMs.

Figure 1 depicts the stylized CCP waterfall considered in our model. The prefunded layers of the default waterfall are included in a solid frame, whereas the last layer (indicated by a dashed frame) represents unfunded resources (we discuss the unfunded layer in more detail when we define the first round of clearing). As mentioned in Faruqui et al. (2018), the skin-in-the-game of the CCP “can come before, along with, and/or after the default fund contributions of non-defaulting members, depending on the CCP's specific rules.” For further discussion on CCPs' default waterfalls, we refer to Cont (2015). In our analysis, the order in which the skin-in-the-game is used relative to the default fund contributions of the surviving members does not matter.

In practice, if a clearing member defaults, its portfolio will be sold by the CCP in an auction (CPMI-IOSCO, 2020). The design of auction mechanisms and their implications have been studied in, for example, Huang and Zhu (2024) and Ferrara et al. (2020). Huang and Zhu (2024) show that juniorization of the guarantee fund contributions of those clearing members that submit bad bids in the auction increases the auction price. In our model, any possible difference in

¹⁵ Huang and Takats (2020) provide empirical evidence that higher skin-in-the-game—even though very limited in size—is associated with more prudent risk management of CCPs (e.g., fewer margin breaches).

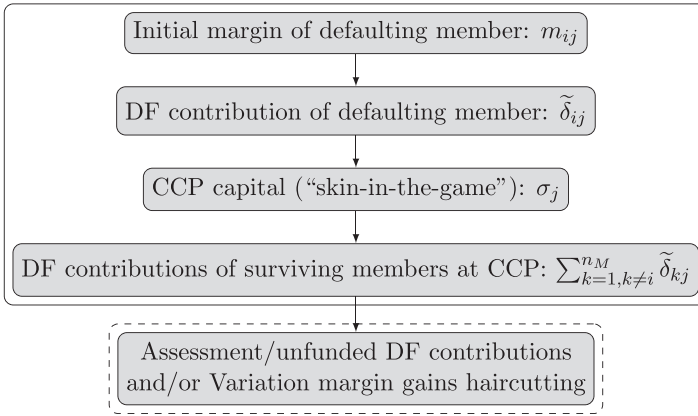


FIGURE 1 A stylized default waterfall of CCP j in a situation where only clearing member i defaults. The first four layers (included in a solid frame) are the prefunded resources of CCP j . The remaining layer (in a dashed frame) indicates unfunded resources of CCP j .

seniority of the guarantee fund contributions of the surviving members will not affect the contagion mechanism, since we assume that each CCP i will use its full resources b_i (in addition to the IMs that correspond to defaulted positions) before it transmits any losses to clearing members directly. We will, therefore, not consider aspects of mechanism design in our contagion model.

First round price-payment-equilibrium: We are now interested in determining a price-payment equilibrium in the first clearing round ($R1$), that is, we aim to determine an $N \times N$ -matrix $p^{*,R1}$, where each component $p_{ij}^{*,R1}$ represents the VM payments made from i to j . In addition, some collateral will need to be liquidated if defaults occur, potentially affecting its market price. Accordingly, we also aim to determine the price $\pi^{*,R1}$ of the collateral in equilibrium. To do so, we consider an inverse demand function modeled along the lines of Cifuentes et al. (2005) which returns the price of the collateral as a function of the amount of collateral sold.¹⁶ The price-payment equilibrium can be characterized by a suitable fixed point. Considering a function $\Phi^{R1} : [0, 1] \times [0, \bar{p}^{R1}] \rightarrow [0, 1] \times [0, \bar{p}^{R1}]$, the goal is to obtain a fixed point of this function, that is, we want to find $(\pi^{*,R1}, p^{*,R1})$ such that

$$(\pi^{*,R1}, p^{*,R1}) = \Phi^{R1}(\pi^{*,R1}, p^{*,R1}).$$

Here, Φ^{R1} is defined as follows:

$$\begin{aligned} \Phi_1^{R1}(\pi, p) &= \exp(-\alpha \Delta(\pi, p)), \\ \Phi_{2,(ij)}^{R1}(\pi, p) &= \begin{cases} \min \left\{ \bar{p}_{ij}^{R1}, \pi m_{ij} + a_{ij}^{R1}(\pi) \left(\gamma_i^{(1)} b_i + \gamma_i^{(2)} \sum_{k=1}^N p_{ki} \right) \right\}, & \text{if } i \in D(p), \\ \bar{p}_{ij}^{R1}, & \text{if } i \in \mathcal{N} \setminus D(p), \end{cases} \end{aligned} \quad (1)$$

where

$$D(p) = \{i \in \mathcal{N} \mid A_i(p) < \bar{p}_i^{R1}\},$$

¹⁶ We use an exponential inverse demand function, which is a common choice in the fire sales literature. It was used by Cifuentes et al. (2005) in a financial contagion model in which illiquid assets are sold to satisfy payment obligations and it has also been used in several other contagion models since then including, for example, by Ghamami et al. (2022). An alternative to an exponential price impact, would be, for example, a linear price impact, as considered by Greenwood et al. (2015).

specifies the nodes in default in a system with payments $p \in [0, \bar{p}^{R1}]$, that is, these are the nodes that have fewer assets than payment obligations, where $A_i(p) = b_i + \sum_{k=1}^N p_{ki}$ denotes the available assets of node $i \in \mathcal{N}$.

In the following, we describe the parameters used in Equation (1) by considering Φ_1^{R1} first, and then Φ_2^{R1} .

Φ_1^{R1} models the inverse demand function for the price of the illiquid collateral. The constant $\alpha \geq 0$ models the price impact of (fire) sales of collateral.¹⁷ If $\alpha = 0$, then there is no price impact and $\Phi_1^{R1}(\pi, p) = 1$ for all $p \in [0, \bar{p}^{R1}]$ and for all $\pi \in [0, 1]$. If $\alpha > 0$ and $\Delta(\pi, p) > 0$, then $\Phi_1^{R1}(\pi, p) < 1$ for all $p \in [0, \bar{p}^{R1}]$ and for all $\pi \in [0, 1]$, hence capturing the decline in the price of collateral when the number of shares $\Delta(\pi, p)$ of collateral is sold. In particular, $\Delta(\pi, p)$ is given by

$$\Delta(\pi, p) = \sum_{i=1}^N \sum_{j=1}^N \Delta_{ij}(\pi, p),$$

where the total shares of collateral seized and sold by node j after the default of node i is given by

$$\Delta_{ij}(\pi, p) = \begin{cases} \min \left\{ m_{ij}, \frac{\bar{p}_{ij}^{R1}}{\pi} \right\}, & \text{if } i \in D(p), \\ 0, & \text{if } i \in \mathcal{N} \setminus D(p), \end{cases}$$

if $\pi > 0$, and when $\pi = 0$, it is given by

$$\Delta_{ij}(\pi, p) = \begin{cases} m_{ij}, & \text{if } i \in D(p) \text{ and } \bar{p}_{ij}^{R1} > 0, \\ 0, & \text{otherwise.} \end{cases}$$

Hence, only collateral of nodes that default (i.e., which are in $D(p)$) can in principle be sold. The number of shares of collateral sold is capped by the collateral available for a given position m_{ij} and by the payment obligations due relative to the price of the collateral.

Φ_2^{R1} models the payments made between the nodes. If a node i does not default then it pays \bar{p}_{ij}^{R1} to a node j . If i does default, it will never pay more to j than its original payment obligation \bar{p}_{ij}^{R1} and it uses the value of its collateral πm_{ij} and parts of its liquidity buffer and payments made by other banks to pay other nodes. In particular, the matrix $a^{R1}(\pi) \in [0, 1]^{N \times N}$ specifies the repayment proportions and it is given by

$$a_{ij}^{R1}(\pi) = \begin{cases} \frac{\max\{0, \bar{p}_{ij}^{R1} - \pi m_{ij}\}}{\sum_{k=1}^N \max\{0, \bar{p}_{ik}^{R1} - \pi m_{ik}\}}, & \text{if } \sum_{k=1}^N \max\{0, \bar{p}_{ik}^{R1} - \pi m_{ik}\} > 0, \\ 0 & \text{otherwise,} \end{cases}$$

¹⁷ For a discussion and further results related to the choice of the parameter α for the exponential inverse demand function, we refer to Amini et al. (2016). In particular, they show that the function modeling the cash proceeds from liquidation $\Delta \mapsto \Delta \exp(-\alpha\Delta)$ is increasing in $[0, \Delta_{\text{total}}]$ if and only if $\alpha \leq \frac{1}{\Delta_{\text{total}}}$. Here, $\Delta_{\text{total}} > 0$ denotes the maximum collateral available for sale, that is, $\Delta_{\text{total}} = \sum_{i=1}^N \sum_{j=1}^N m_{ij}$. In the following, we will always choose α such that this condition is satisfied.

for all $i, j \in \mathcal{N}$, where $a_{ij}^{\text{RI}}(\pi)$ specifies the relative payment obligations due from i to j while accounting for IMs. In other words, $a_{ij}^{\text{RI}}(\pi)$ describes the relative payment obligations from i to j that are not covered by collateral (i.e., IMs) when the price of the collateral per share is π .

The parameters $\gamma_i^{(1)}, \gamma_i^{(2)} \in [0, 1]$, $i \in \mathcal{N}$ are used to model exogenous default costs (Rogers & Veraart, 2013) and the severity of VMGH, respectively. When $\gamma_i^{(1)} < 1$ or $\gamma_i^{(2)} < 1$, we can capture the effect that, in case of default, not all assets are available or used to pay counterparties. In the special case where $\gamma_1^{(1)} = \dots = \gamma_N^{(1)} = 1$ and $\gamma_1^{(2)} = \dots = \gamma_N^{(2)} = 1$, the first round mathematically corresponds to the model in Ghamami et al. (2022).

The parameters $\gamma_i^{(1)}, \gamma_i^{(2)}$, $i \in \mathcal{N}$ only play a role if there are defaulting nodes. Every node i that defaults (i.e., is in $\mathcal{D}(p)$), uses the proportion $\gamma_i^{(1)}$ of its liquidity buffer b_i and the proportion $\gamma_i^{(2)}$ of the payments it received ($\sum_{k=1}^N p_{ki}$) to make payments to other nodes. How much an individual node j receives from i is determined both by the proportion $a_{ij}^{\text{RI}}(\pi)$, which is used to distribute the cash available to j , and the IM evaluated at the market price πm_{ij} .

If a node $i \in \mathcal{D}(p)$ is a CCP¹⁸, then, formula (1) simplifies to

$$\Phi_{2,(ij)}^{\text{RI}}(\pi, p) = \min \left\{ \bar{p}_{ij}^{\text{RI}}, \frac{\bar{p}_{ij}^{\text{RI}}}{\bar{p}_i^{\text{RI}}} \left(\gamma_i^{(1)} b_i + \gamma_i^{(2)} \sum_{k=1}^N p_{ki} \right) \right\},$$

since CCPs do not post IM to their clearing members. In particular, the payments of CCP i to its clearing members do not directly depend on the price of the collateral π .

For each CCP i , we will assume that $\gamma_i^{(1)} = 1$, which means that the full prefunded resources from the default waterfall b_i are used to make payments to its clearing members.

If all prefunded resources are not enough to meet its payment obligations, then we think of CCP i as being in default (i.e., $i \in \mathcal{D}(p)$). What this implies is that not all due payments are made in full. In this case, we distinguish two subcases, which we refer to as variants of VMGH. The severity of the VMGH is modeled by the parameter $\gamma_i^{(2)}$. If $\gamma_i^{(2)} = 1$, then node i pays out the full amount of VMs received from its clearing members to clearing members to which payments are due, but this is still not enough to meet payment obligations—we refer to this situation as one of *soft* VMGH. If $\gamma_i^{(2)} < 1$, however, then node i does not pay out the full amount of VMs received to clearing members to which payments are due—a situation we refer to as *severe* VMGH.¹⁹ In practice, VMGH is done pro rata (Gregory, 2014) and this is captured by the proportion $\frac{\bar{p}_{ij}^{\text{RI}}}{\sum_{k=1}^N \bar{p}_{ik}^{\text{RI}}}$.

For each clearing member i , we will also consider different choices of $\gamma_i^{(1)}, \gamma_i^{(2)}$. In particular, $\gamma_i^{(1)} = \gamma_i^{(2)} = 1$ would correspond to a *soft* default and $\gamma_i^{(1)} = \gamma_i^{(2)} = 0$ would correspond to a *hard* default of the clearing member, as in Paddrik and Young (2021). We will allow for intermediate cases, that is, $\gamma_i^{(1)}, \gamma_i^{(2)} \in (0, 1)$ as well.

The introduction of the parameters $\gamma_i^{(1)}, \gamma_i^{(2)} \in [0, 1]$, $i \in \mathcal{N}$ has implications for the fire sale of collateral as well. If some of these parameters are strictly smaller than one, this can increase the losses spreading through the system. If those losses cause additional defaults of clearing members, then more collateral will be liquidated, causing a stronger price decline of the collateral, which itself can feed back to further losses and defaults. Therefore, these two channels interact and can amplify the contagion effects.

¹⁸ Since $i \in \mathcal{D}(p)$, we have that $\sum_{k=1}^N \bar{p}_{ik}^{\text{RI}} > 0$.

¹⁹ Strictly speaking, this second variant is closer to VMGH as commonly discussed.

Using Tarksi’s fixed point theorem, we show in Appendix A that the set of fixed points of the function Φ^{R1} is a nonempty complete lattice. Throughout this paper, we will always consider the greatest fixed point of Φ^{R1} and denote this by $(\pi^{*,R1}, p^{*,R1})$.²⁰

Definition 2.1 (Defaults). We will refer to all nodes in the set

$$D(p^{*,R1}) = \left\{ i \in \mathcal{N} \mid A_i(p^{*,R1}) < \bar{p}_i^{R1} \right\} = \left\{ i \in \mathcal{N} \mid b_i + \sum_{k=1}^N p_{ki}^{*,R1} < \bar{p}_i^{R1} \right\}$$

as *nodes in default*. We refer to all nodes in the set $\mathcal{F} = D(\bar{p}^{R1}) = \{i \in \mathcal{N} \mid b_i + \sum_{k=1}^N \bar{p}_{ki}^{R1} < \bar{p}_i^{R1}\}$ as *fundamental defaults*. We refer to all nodes in the set $D(p^{*,R1}) \setminus \mathcal{F}$ as *contagious defaults*.

Hence, all nodes that cannot satisfy their payment obligations even if all other nodes satisfy theirs are referred to as fundamental defaults. We show in Corollary A.3 in the Appendix that $\mathcal{F} \subseteq D(p^{*,R1})$.

Remark 2.2 (No fundamental defaults among CCPs). CCPs have matched books, that is, for each $i \in C$, it holds that $\sum_{k=1}^N \bar{p}_{ki}^{R1} = \bar{p}_i^{R1}$, which means that the total variation margins that $i \in C$ is due to pay (\bar{p}_i^{R1}) coincide with the variation margin payments that the clearing members are due to pay to CCP i (namely, $\sum_{k=1}^N \bar{p}_{ki}^{R1}$). This implies (together with $b_i \geq 0$ for all $i \in C$), that the set of fundamental defaults \mathcal{F} cannot contain CCPs, that is, $\mathcal{F} \cap C = \emptyset$.

Second round price-payment equilibrium: Next, we consider the same mechanism for a second round of clearing ($R2$), as proposed in Ghamami et al. (2022). The main idea of the second round of clearing is that collateral not used in the first round is freed and becomes available to make still-outstanding payments. This can be modeled by considering a second fixed point problem.

Let $(\pi^{*,R1}, p^{*,R1}) \in [0, 1] \times [0, \bar{p}^{R1}]$ be the greatest fixed point of Φ^{R1} defined in Equation (1). Then, the payments that are still outstanding at the start of the second round are given by $\bar{p}^{R2} = \bar{p}^{R1} - p^{*,R1} \in [0, \bar{p}^{R1}]$. We define a function $\Phi^{R2} : [0, \pi^{*,R1}] \times [0, \bar{p}^{R2}] \rightarrow [0, \pi^{*,R1}] \times [0, \bar{p}^{R2}]$ and the aim is to determine a fixed point of this function, that is, we want to find $(\pi^{*,R2}, p^{*,R2})$ such that

$$(\pi^{*,R2}, p^{*,R2}) = \Phi^{R2}(\pi^{*,R2}, p^{*,R2}),$$

where

$$\begin{aligned} \Phi_1^{R2}(\pi, p) &= \pi^{*,R1} \exp(-\alpha\Gamma(\pi, p)), \\ \Phi_{2,(ij)}^{R2}(\pi, p) &= \min \left\{ \bar{p}_{ij}^{R2}, a_{ij}^{R2} \left(\pi r_i(\pi^{*,R1}, p^{*,R1}) + \sum_{k=1}^N p_{ki} \right) \right\}, \end{aligned} \tag{2}$$

²⁰ It would be possible to also consider the least fixed point, which can arise as the outcome of a decentralized clearing mechanism, see, for example, Csóka and Herings (2018). For example, Bardoscia et al. (2019) provide a payment algorithm in which market participants delay their payments under liquidity stress. Such a strategic response corresponds to a special least fixed point, see Veraart and Zhang (2021) for further details.

and

$$a_{ij}^{\text{R2}} = \begin{cases} \frac{\bar{p}_{ij}^{\text{R2}}}{\sum_{k=1}^N \bar{p}_{ik}^{\text{R2}}}, & \text{if } \sum_{k=1}^N \bar{p}_{ik}^{\text{R2}} > 0, \\ 0, & \text{otherwise,} \end{cases}$$

denotes the repayment proportions for $i, j \in \mathcal{N}$ in the second round. Here, $\Gamma(\pi, p)$ denotes the total shares of collateral sold in the second round, that is,

$$\Gamma(\pi, p) = \sum_{i=1}^N \Gamma_i(\pi, p),$$

where the total shares of collateral sold by node $i \in \mathcal{N}$ is given by

$$\Gamma_i(\pi, p) = \min \left\{ r_i(\pi^{*,\text{R1}}, p^{*,\text{R1}}), \frac{1}{\pi} \max \left\{ 0, \sum_{j=1}^N \bar{p}_{ij}^{\text{R2}} - \sum_{j=1}^N p_{ji} \right\} \right\},$$

if $\pi > 0$. For $\pi = 0$, we set

$$\Gamma_i(\pi, p) = \begin{cases} r_i(\pi^{*,\text{R1}}, p^{*,\text{R1}}), & \text{if } i \in \mathcal{D}(p^{*,\text{R1}}) \text{ and } \sum_{j=1}^N \bar{p}_{ij}^{\text{R2}} > \sum_{j=1}^N p_{ji}, \\ 0, & \text{otherwise.} \end{cases}$$

Furthermore, $r_i(\pi^{*,\text{R1}}, p^{*,\text{R1}})$ is the collateral returned to node $i \in \mathcal{N}$ and is defined as

$$r_i(\pi^{*,\text{R1}}, p^{*,\text{R1}}) = \begin{cases} \sum_{j=1}^N (m_{ij} - \Delta_{ij}(\pi^{*,\text{R1}}, p^{*,\text{R1}})), & \text{if } i \in \mathcal{D}(p^{*,\text{R1}}), \\ \sum_{j \in \mathcal{D}(p^{*,\text{R1}})} m_{ij}, & \text{if } i \in \mathcal{N} \setminus \mathcal{D}(p^{*,\text{R1}}). \end{cases}$$

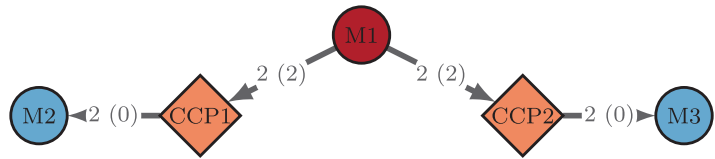
In our setting, the market consists of clearing members and CCPs. Since we assume that CCPs do not post IMs to their clearing members, only clearing members can have collateral returned to them in Round 2. In particular, this implies that $r_i(\pi^{*,\text{R1}}, p^{*,\text{R1}}) = 0$ for all $i \in \mathcal{C}$.

The existence of a greatest fixed point of Φ^{R2} for the second round of clearing follows directly from Ghamami et al. (2022, Proposition 3.1), in addition to the arguments provided in the Appendix for the modified first round of clearing. We denote the greatest fixed point of Φ^{R2} by $(\pi^{*,\text{R2}}, p^{*,\text{R2}})$.

The second round of clearing can only increase payments made between the nodes compared to the first round. It will not affect which nodes default since defaults are solely determined in the first round by looking at available assets to make payments, see Definition 2.1.²¹

²¹ It is possible that for a node $i \in \mathcal{D}(p^{*,\text{R1}})$, it holds that $\bar{p}_{ij}^{\text{R1}} = p_{ij}^{*,\text{R1}} + p_{ij}^{*,\text{R2}}$ for all $j \in \mathcal{N}$, that is, it satisfies its obligations in full once its collateral is seized and used to compensate for shortfalls. In particular, the actual payments made between institutions cannot reveal whether an institution defaults or not, since the default event can make additional resources available (the collateral), see Ghamami et al. (2022) for further discussion. A similar situation also arises in Kusnetsov and Veraart (2019) in a setting with multiple maturities, and in Banerjee and Feinstein (2019) in a network with contingent payments.

FIGURE 2 Example #1—Default of a joint clearing member affecting several CCPs. Color code: fundamental defaults (red), clearing members not in fundamental default (blue), CCPs (orange). [Color figure can be viewed at wileyonlinelibrary.com]



Remark 2.3 (Seniority of payments). The definitions of Φ^{R1} and Φ^{R2} reflect the fact that all payment obligations have the same seniority. It is possible to change this assumption to allow, for example, for situations in which clearing members pay CCPs according to a pecking order rather than based on a proportionality assumption. In Appendix C, we discuss this modification in detail. While this change in clearing method will lead to different price-payment equilibria, we show that the key insights developed in this paper remain the same under both types of clearing mechanisms.

3 | JOINT CLEARING MEMBERS AND LOSS TRANSMISSION

With the fundamentals of the model behind us, we now provide stylized examples that illustrate different types of loss transmissions arising from multiple CCPs with joint clearing members. To do this, we compute the clearing payments and clearing price of the collateral in both rounds and consider the pair-specific payment shortfalls S_{ij} , where $i, j \in \mathcal{N}$, after the two rounds of clearing, given by

$$S_{ij} = \max \left\{ 0, \bar{p}_{ij}^{R1} - p_{ij}^{*,R1} - p_{ij}^{*,R2} \right\}, \quad i, j \in \mathcal{N},$$

and the total payment shortfall S , which measures the amount of unfulfilled payment obligations after the two clearing rounds (using the IMs where applicable), defined as

$$S = \sum_{i=1}^N \sum_{j=1}^N S_{ij}.$$

Furthermore, we define the relative payment shortfall as S_{ij}/\bar{p}_{ij}^{R1} for all $i, j \in \mathcal{N}$ and the total relative payment shortfall as $S/\sum_{i=1}^N \sum_{j=1}^N \bar{p}_{ij}^{R1}$. The relative payment shortfall and the total relative payment shortfall take values in $[0, 1]$ and capture payment shortfalls relative to payment obligations.

3.1 | Example #1: Default of a joint clearing member

First, we consider the situation where a joint clearing member defaults simultaneously at two CCPs. We show that this can result in both CCPs suffering severe losses and could potentially even cause their default if the collateral posted by the defaulting clearing member is illiquid.

We consider a system consisting of $n_C = 2$ CCPs and $n_M = 3$ clearing members. Figure 2 provides an illustration of the network of payment obligations. The weights along the edges represent

the payment obligation due from i to j in the first round, that is, \bar{p}_{ij}^{R1} , and the numbers in parentheses represent the corresponding IMs (m_{ij}). For simplicity, we assume that the liquidity buffers are zero, but the example can be easily generalized to include positive liquidity buffers, default funds, and skin-in-the-game.

There is one joint clearing member (M1) that clears at both CCPs. The other two clearing members only clear at one CCP each (M2 at CCP1 and M3 at CCP2). We label the clearing members M_i with index i for $i \in \{1, 2, 3\}$, CCP1 with index 4 and CCP2 with index 5 in the matrices and vectors below.

Formally,

$$\bar{p}^{R1} = \begin{pmatrix} 0 & 0 & 0 & 2 & 2 \\ 0 & 0 & 0 & 0 & 0 \\ 0 & 0 & 0 & 0 & 0 \\ 0 & 2 & 0 & 0 & 0 \\ 0 & 0 & 2 & 0 & 0 \end{pmatrix}, \quad m = \begin{pmatrix} 0 & 0 & 0 & 2 & 2 \\ 0 & 0 & 0 & 0 & 0 \\ 0 & 0 & 0 & 0 & 0 \\ 0 & 0 & 0 & 0 & 0 \\ 0 & 0 & 0 & 0 & 0 \end{pmatrix}, \quad b = (0, 0, 0, 0, 0)^\top.$$

The joint clearing member M1 is the only node in fundamental default, that is, $\mathcal{F} = \{1\} = \{M1\}$. We assume that $\gamma_i^{(1)}, \gamma_i^{(2)} \in [0, 1]$ for all $i \in \mathcal{N}$. We consider various cases.

1. First, we consider the case of fully liquid collateral that can be liquidated at no discount, that is, $\alpha = 0$.

In this scenario, the price of the collateral cannot change, that is, $\pi^{*,R1} = \pi^{*,R2} = 1$. Furthermore, we obtain that $p^{*,R1} = \bar{p}^{R1}$ and $p^{*,R2} = 0$, implying that all payments are made in full (the total shortfall is $S = 0$). Here, $\mathcal{D}(p^{*,R1}) = \mathcal{F} = \{1\}$. Hence, even though clearing member M1 is in fundamental default, CCP1 still receives 2 from M1 by seizing the IM $m_{14} = 2$ and the same situation arises for CCP2, which seizes $m_{15} = 2$. Therefore, both CCP1 and CCP2 are able to satisfy their payment obligations of 2 to M2 and M3, respectively, in full.

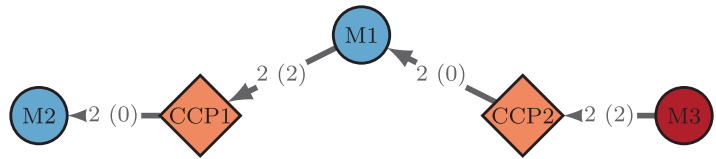
Note that in this example, the values of $\gamma_i^{(1)}$ and $\gamma_i^{(2)}$ do not matter, since the joint clearing member M1 does not pay the CCPs directly (these payments would be affected by the parameters $\gamma_i^{(1)}, \gamma_i^{(2)}$) as it does not have any resources to use. The CCPs seize the IMs instead, and therefore the clearing payments $p^{*,R1} = \bar{p}^{R1}$ correspond to the full payment obligations in Round 1 and there is nothing left to be paid in Round 2, that is, $p^{*,R2} = 0$.

2. Second, we assume that the collateral is illiquid by setting $\alpha = 0.25 > 0$. The total shares of collateral sold in the first round are $\Delta = 4$, and in the second round $\Gamma = 0$. Furthermore, the clearing price of the collateral in both rounds is given by $\pi^{*,R1} = \pi^{*,R2} = \exp(-4\alpha) \approx 0.3679$. It does not decrease from the first to the second round, since no collateral is sold in the second round in this case. The clearing payments in the first round are given by

$$p^{*,R1} = \begin{pmatrix} 0 & 0 & 0 & 2\pi^{*,R1} & 2\pi^{*,R1} \\ 0 & 0 & 0 & 0 & 0 \\ 0 & 0 & 0 & 0 & 0 \\ 0 & \gamma_4^{(2)} 2\pi^{*,R1} & 0 & 0 & 0 \\ 0 & 0 & \gamma_5^{(2)} 2\pi^{*,R1} & 0 & 0 \end{pmatrix}$$

and the clearing payments in the second round are given by the zero matrix, that is, $p^{*,R2} = 0$.

FIGURE 3 Example #2—Loss transmission due to joint clearing members network. Color code as in Figure 2. [Color figure can be viewed at wileyonlinelibrary.com]



This implies that the total shortfall is $S = 2(2 - 2\pi^{*,R1}) + (2 - 2\gamma_4^{(2)}\pi^{*,R1}) + (2 - 2\gamma_5^{(2)}\pi^{*,R1})$. In particular, the total shortfall depends on $\gamma_i^{(2)}$, $i \in \{4, 5\}$. For example, for $\gamma_4^{(2)} = \gamma_5^{(2)} = 1$, $S \approx 5.057$ and for $\gamma_4^{(2)} = \gamma_5^{(2)} = 0.5$, $S \approx 5.793$.

Furthermore, for all choices of $\gamma_4^{(2)}, \gamma_5^{(2)}$, both CCPs suffer a contagious default and $D(p^{*,R1}) = \{1, 4, 5\}$. Hence, even though the liabilities of the joint clearing member were fully collateralized at both CCPs, the fact that this collateral was illiquid still caused the (contagious default) of both CCPs, which caused knock-on losses to clearing members that only clear at one CCP.

The scenario from this stylized example has been considered by Glasserman et al. (2015) before, but not in the context of a model involving different contagion channels. They show that convex IM schedules provide incentives for clearing members to split their positions across multiple CCPs. This gives rise to what they refer to as *hidden illiquidity*—that is, the CCPs involved are not aware that the positions of some of their joint clearing members are in fact undercollateralized.

We demonstrate how this effect can be captured by the different contagion mechanisms in our model. In our example, CCP1 does not know that M1 has the same position at CCP1 and CCP2 and therefore for CCP1, it may appear that the position of M1 is sufficiently collateralized. For illiquid collateral, however, we find that both CCPs can default, and if these two CCPs use more severe VMGH (achieved by setting $\gamma_4^{(2)} = \gamma_5^{(2)} = 0.5$ as in our last example) then other clearing members can suffer substantial additional losses.

3.2 | Example #2: Default of clearing member at only one CCP

Next, we show that even if there is no fundamental default among the joint clearing members, they can still act as a transmission channel of losses from one CCP to another. To illustrate this effect, we consider a situation where there is only one fundamental default in a clearing member that only clears at one CCP.

As before, we consider an example consisting of $n_C = 2$ CCPs and $n_M = 3$ clearing members. Figure 3 provides an illustration of the network of payment obligations. The notation is the same as in Figure 2.

Formally,

$$\bar{p}^{R1} = \begin{pmatrix} 0 & 0 & 0 & 2 & 0 \\ 0 & 0 & 0 & 0 & 0 \\ 0 & 0 & 0 & 0 & 2 \\ 0 & 2 & 0 & 0 & 0 \\ 2 & 0 & 0 & 0 & 0 \end{pmatrix}, \quad m = \begin{pmatrix} 0 & 0 & 0 & 2 & 0 \\ 0 & 0 & 0 & 0 & 0 \\ 0 & 0 & 0 & 0 & 2 \\ 0 & 0 & 0 & 0 & 0 \\ 0 & 0 & 0 & 0 & 0 \end{pmatrix}, \quad b = (0, 0, 0, 0, 0)^T.$$

Here, $\mathcal{F} = \{3\} = \{M3\}$, hence the clearing member (labeled M3 in Figure 3) is the only fundamental default. As in the first example, we consider two alternative cases by varying the liquidity of the collateral.

1. As before, when collateral is liquid (i.e., $\alpha = 0$), the price of collateral cannot change and all payments are made in full (the total shortfall is $S = 0$). There are no contagious defaults and the default set is comprised only of the original fundamental default ($\mathcal{D}(p^{*,R1}) = \mathcal{F} = \{3\} = \{M3\}$), as CCP2 still receives 2 from M3 by seizing the IM $m_{35} = 2$ and is able to satisfy its payment obligations in full. As in the previous example, the value of $\gamma_3^{(2)}$ does not matter, since CCP2 seizes the collateral and there are no other payments from M3 to CCP2 (which would be affected by the parameter $\gamma_3^{(2)}$). Also note that, since $b_3 = 0$, the value of $\gamma_3^{(1)}$ does not matter either.
2. Second, we assume that collateral is illiquid ($\alpha = 0.01 > 0$). In this case, both defaults and shortfall depend on $\gamma_1^{(2)}, \gamma_4^{(2)}, \gamma_5^{(2)}$. In particular, we find that both CCP2 and M1 suffer a contagious default for all choices of $\gamma_i^{(1)}, \gamma_i^{(2)}, i \in \mathcal{N}$, but whether CCP1 suffers a contagious default or not depends on the particular values of $\gamma_1^{(2)}, \gamma_4^{(2)}, \gamma_5^{(2)}$.

For all $\gamma_i^{(1)}, \gamma_i^{(2)} \in [0, 1]$, the total shares of collateral sold are $\Delta = 4, \Gamma = 0$, resulting in prices for the collateral of $\pi^{*,R1} = \pi^{*,R2} = \exp(-4\alpha) \approx 0.9608$. Furthermore,

$$p_{14}^{*,R1} = \min \left\{ 2, 2\pi^{*,R1}(1 + \gamma_1^{(2)}\gamma_5^{(2)}) \right\},$$

$$p_{35}^{*,R1} = 2\pi^{*,R1},$$

$$p_{42}^{*,R1} = \min \left\{ 2, \gamma_4^{(2)} p_{14}^{*,R1} \right\} = \min \left\{ 2, \gamma_4^{(2)} \min \left\{ 2, 2\pi^{*,R1}(1 + \gamma_1^{(2)}\gamma_5^{(2)}) \right\} \right\},$$

$$p_{51}^{*,R1} = \gamma_5^{(2)} 2\pi^{*,R1},$$

and $p_{ij}^{*,R1} = 0$ for the remaining index pairs (i, j) and $p^{*,R2} = 0$. The shortfall is given by

$$S = \left(2 - \min \left\{ 2, 2\pi^{*,R1} \left(1 + \gamma_1^{(2)}\gamma_5^{(2)} \right) \right\} \right) + (2 - 2\pi^{*,R1}) \\ + \left(2 - \min \left\{ 2, \gamma_4^{(2)} \min \left\{ 2, 2\pi^{*,R1} \left(1 + \gamma_1^{(2)}\gamma_5^{(2)} \right) \right\} \right\} \right) + (2 - \gamma_5^{(2)} 2\pi^{*,R1}),$$

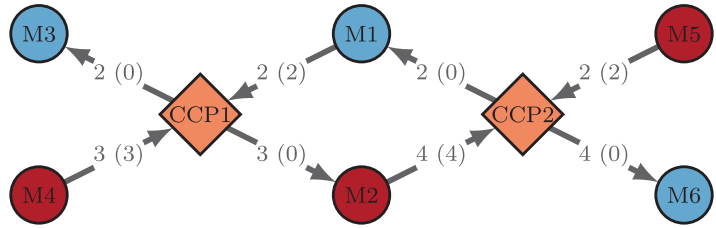
that is, it depends on $\gamma_1^{(2)}, \gamma_4^{(2)}, \gamma_5^{(2)}$. For example, for $\gamma_1^{(2)} = \gamma_4^{(2)} = \gamma_5^{(2)} = 1$, $S \approx 0.1568$ and $\mathcal{D}(p^{*,R1}) = \{1, 3, 5\} = \{M1, M3, CCP2\}$.

If CCP2 does very severe VMGH, achieved by, for example, setting $\gamma_5^{(2)} = 0$ (and $\gamma_1^{(2)} = \gamma_4^{(2)} = 1$), then $S \approx 2.2353$ and $\mathcal{D}(p^{*,R1}) = \{1, 3, 4, 5\} = \{M1, M3, CCP1, CCP2\}$. Hence, there is the additional default of CCP1.

If both CCPs do severe VMGH, by, for example, setting $\gamma_4^{(2)} = \gamma_5^{(2)} = 0$ (and $\gamma_1^{(2)} = 1$), then the total shortfall increases even further to $S \approx 4.1568$, but the default set remains the same, that is, $\mathcal{D}(p^{*,R1}) = \{1, 3, 4, 5\} = \{M1, M3, CCP1, CCP2\}$.

This example serves to illustrate that the default of an institution (M3) can trigger the default of a CCP (CCP1) at which it is not a clearing member. In particular, here the VMGH of CCP2 is one of the causes of the default of CCP1. So, while VMGH can serve as a defense mechanism

FIGURE 4 Example #3—Cycle of loss transmission due to joint clearing members network. Color code as in Figure 2. [Color figure can be viewed at wileyonlinelibrary.com]



for CCP2 on a stand-alone basis, it can have contagion effects and ultimately lead to the default of another CCP.

3.3 | Example #3: Circular loss transmission via joint clearing members and multiple CCPs

Finally, we consider a situation with multiple joint clearing members that create a circle of loss transmission between them and CCPs, which can cause the default of both types of institutions. We still consider a system with $n_C = 2$ CCPs, but now have $n_M = 6$ clearing members. Figure 4 provides an illustration of the network of payment obligations. The notation is the same as in Figure 2. In contrast to the previous examples, we now consider two joint clearing members that clear at both CCPs, which leads to a circular structure of payment obligations.

Formally,

$$\bar{p}^{R1} = \begin{pmatrix} 0 & 0 & 0 & 0 & 0 & 0 & 2 & 0 \\ 0 & 0 & 0 & 0 & 0 & 0 & 0 & 4 \\ 0 & 0 & 0 & 0 & 0 & 0 & 0 & 0 \\ 0 & 0 & 0 & 0 & 0 & 0 & 3 & 0 \\ 0 & 0 & 0 & 0 & 0 & 0 & 0 & 2 \\ 0 & 0 & 0 & 0 & 0 & 0 & 0 & 0 \\ 0 & 3 & 2 & 0 & 0 & 0 & 0 & 0 \\ 2 & 0 & 0 & 0 & 0 & 0 & 0 & 4 \end{pmatrix}, \quad m = \begin{pmatrix} 0 & 0 & 0 & 0 & 0 & 0 & 2 & 0 \\ 0 & 0 & 0 & 0 & 0 & 0 & 0 & 4 \\ 0 & 0 & 0 & 0 & 0 & 0 & 0 & 0 \\ 0 & 0 & 0 & 0 & 0 & 0 & 3 & 0 \\ 0 & 0 & 0 & 0 & 0 & 0 & 0 & 2 \\ 0 & 0 & 0 & 0 & 0 & 0 & 0 & 0 \\ 0 & 0 & 0 & 0 & 0 & 0 & 0 & 0 \\ 0 & 0 & 0 & 0 & 0 & 0 & 0 & 0 \end{pmatrix}, \quad b = (0, 0, 0, 0, 0, 0, 0, 0)^T. \tag{3}$$

There are three fundamental defaults, $\mathcal{F} = \{2, 4, 5\} = \{M2, M4, M5\}$. The node M4 is only a clearing member of CCP1, the node M5 is only a clearing member of CCP2 and the node M2 is a joint clearing member of both CCPs, but only has payment obligations to CCP2. As before, we consider alternative cases:

1. We first consider the case of liquid collateral, that is, $\alpha = 0$. We now distinguish between two subcases: fully versus not fully collateralized obligations from clearing members to CCPs.
 - (a) Fully collateralized obligations correspond to the IMs given by m in Equation (3). In this case, $p^{*,R1} = \bar{p}^{R1}$ and $p^{*,R2} = 0$: all payments are made in full and the total shortfall is zero. Collateral sold amounts to $\Delta = 9$ in the first round and $\Gamma = 0$ in the second round. There are, thus, no contagious defaults ($D(p^{*,R1}) = \mathcal{F}$). As in previous examples, the values of $\gamma_i^{(1)}, \gamma_i^{(2)}$ do not matter in this case.

- (b) If we reduce IMs by considering $0.99m$ rather than m in Equation (3), the situation changes. Fundamental defaults remain the same, but the overall default set is larger. In particular, $D(p^{*,R1}) = \{M1, M2, M4, M5, CCP1, CCP2\}$, that is, both CCPs and the additional joint clearing member M1 default as well (even for $\gamma_i^{(1)} = \gamma_i^{(2)} = 1$ for all $i \in \mathcal{N}$).

The total shortfall depends on the parameters $\gamma_i^{(1)}, \gamma_i^{(2)}$. For example, for $\gamma_i^{(1)} = \gamma_i^{(2)} = 1$ for all $i \in \mathcal{N}$, the total shortfall is $S = 0.1$, whereas for $\gamma_7^{(2)} = \gamma_8^{(2)} = 0.5$ (and $\gamma_i^{(1)} = 1$ for all $i \in \mathcal{N}$ and $\gamma_i^{(2)} = 1$ for all $i \in \mathcal{M}$), the shortfall increases to $S = 5.575$. In this example, the collateral sold is $\Delta = 11 \cdot 0.99 = 10.89$ in the first round and $\Gamma = 0$ in the second round.

2. Second, we assume that collateral is illiquid ($\alpha > 0$). We further assume that IMs are given by m in Equation (3), that is, payment obligations of clearing members to the CCPs are fully collateralized. We then consider two subcases, based on differences in liquidity buffers.

- (a) First, we consider a liquidity buffer of 0 for all nodes, that is, b as given in Equation (3). For all $\gamma_i^{(1)}, \gamma_i^{(2)} \in [0, 1]$, $i \in \mathcal{N}$, collateral sold in the two rounds is given by $\Delta = 11$ and $\Gamma = 0$, with corresponding collateral price $\pi^{*,R1} = \pi^{*,R2} = \exp(-11\alpha)$. For $\alpha = -\frac{\log(0.99)}{\Delta} \approx 0.00091$, that is, one obtains the same outcome as in 1(b) above. In other words, for $\gamma_i^{(1)} = \gamma_i^{(2)} = 1$ for all $i \in \mathcal{N}$, the shortfall is $S = 0.1$, whereas for $\gamma_7^{(2)} = \gamma_8^{(2)} = 0.5$ (and $\gamma_i^{(1)} = 1$ for all $i \in \mathcal{N}$ and $\gamma_i^{(2)} = 1$ for all $i \in \mathcal{M}$), the shortfall increases to $S = 5.575$ and again $D(p^{*,R1}) = \{M1, M2, M4, M5, CCP1, CCP2\}$.

- (b) Second, we increase the liquidity buffers of two nodes. For members M2 and M4, we take the buffers to $b_2 = 1$ and $b_4 = 3$, respectively, which ensures that neither of them is in the fundamental default set, now given by $\mathcal{F} = \{M5\}$.

With $\alpha = 0.1$ and $\gamma_i^{(1)} = \gamma_i^{(2)} = 1$ for all $i \in \mathcal{N}$, the fundamental default of M5 causes the contagious default of CCP2 and the joint clearing member M1, that is, $D(p^{*,R1}) = \{M1, M5, CCP2\}$, and the shortfall amounts to $S \approx 1.3187$. Still, CCP1 does not default.

Changing $\gamma_8^{(2)} = 1$ to $\gamma_8^{(2)} = 0.25$, that is, assuming that CCP2 uses more severe VMGH (while keeping all other parameters the same), yields $D(p^{*,R1}) = \{M1, M2, M5, CCP1, CCP2\}$ and the shortfall increases to $S \approx 7.2629$. Hence, more severe VMGH by CCP2 triggers the default of CCP1 and the joint clearing member M2.

This example shows that insufficient collateral, either because it was not posted in the first place (example 1b)) or because it is illiquid (example 2a)), can cause contagion and defaults of CCPs. Example 2(b) shows how the default of a clearing member (M5) at one CCP (CCP2) can ultimately trigger the default of another CCP (CCP1) of which M5 is not a clearing member, conditional on the first affected CCP (CCP2) using VMGH. This then triggers the default of M2, in turn leading to further losses at CCP2 due to the circular structure arising from joint clearing membership.

3.4 | Joint clearing members and trapped liquidity

So far, we have assumed that when VMs become due, both clearing members and CCPs make these payments at the same time. In practice, however, this might not be the case. As described in ESRB (2020, p. 51), “CCPs typically only pay out VM gains to counterparties the next morning [...]. In times of high market volatility, this practice results in liquidity being trapped in CCPs and could create or amplify liquidity stress in the financial system.” In the following, we will illustrate

the consequences of trapped liquidity in situations with joint clearing members, revisiting the previous three examples.

In Example 3.1 (default of a joint clearing member, M1), the effects of trapped liquidity in the two CCPs would imply that clearing members M2 and M3 would not receive any payments at time 1, since both CCPs withhold their payments. But since clearing members M2 and M3 do not have any payment obligations, there is no further contagion. In Example 3.2, the payment delays of CCP2 can have consequences for CCP1, as joint clearing member M1 is due to receive payments from CCP2 and must make payments to CCP1. Suppose we equip clearing member M3 with a liquidity buffer of 2. Then, if all VM gains are passed through all CCPs simultaneously, there are no defaults. If only clearing members make payments, however, then clearing member M1 only has its liquidity buffer (assumed to be 0) available to make the required VM payments of 2 to CCP1 and hence cannot meet this payment. A joint clearing member with a matched book can, therefore, become a source of liquidity stress to a CCP (here CCP2) due to another CCP (here CCP1) not passing through its VM gains.

This mechanism (i.e., joint clearing members becoming a liquidity stress to a CCP), can occur repeatedly if we have a circular structure as in Example 3.3.

4 | EMPIRICAL EVIDENCE FOR THE INTERCONNECTEDNESS OF CENTRALLY CLEARED MARKETS

We now present empirical evidence for the interconnectedness of centrally cleared markets. The presence of CCPs affects financial interconnections in various ways. The most obvious, and the one that has attracted the most attention, is the reconfiguration of the financial network to a star-shaped form—whereby the CCP stands in the middle as a large node centralizing all traffic. While useful as a focal point to think about how CCPs affect the nature of counterparty and liquidity risks, this is still a stylized representation. In practice, the CCP ecosystem gives rise to layers of interconnections. As discussed above, CCP membership consists of a reduced group of large financial institutions that simultaneously clears in multiple CCPs. Quite often, these same institutions will provide additional services to CCPs giving rise to further interconnections, such as liquidity provision, credit lines, and custodianship (BCBS-CPMI-FSB-IOSCO, 2018).

Figures 5 and 6 present two key stylized facts that informed our modeling. Figure 5 captures the time series of notional amounts cleared by different CCPs in IRS and CDS markets. While concentrated, both markets feature a few CCPs, that is, the network is not exactly star-shaped. Moreover, some CCPs clear in both markets, whereas others do so only in one market. Figure 6 in turn captures the bipartite network of clearing members (left) and CCPs (right). An edge between a clearing member and a CCP indicates that the member clears at this particular CCP. As is evident, there is a strong overlap between the clearing members at multiple CCPs.

Next, we further investigate the overlap in clearing membership through one-mode projections. One-mode projections are a way to condense information in bipartite networks.²² While the original bipartite network consists of two types of nodes (clearing members and CCPs), a one-mode projection projects this bipartite network onto a network that consists only of one of the two groups. Edges appear between the nodes in the new network if there is a relationship between those two nodes in the dimension that is no longer directly visible. So an edge in the network of

²² For background on one-mode projections, see Newman (2010).

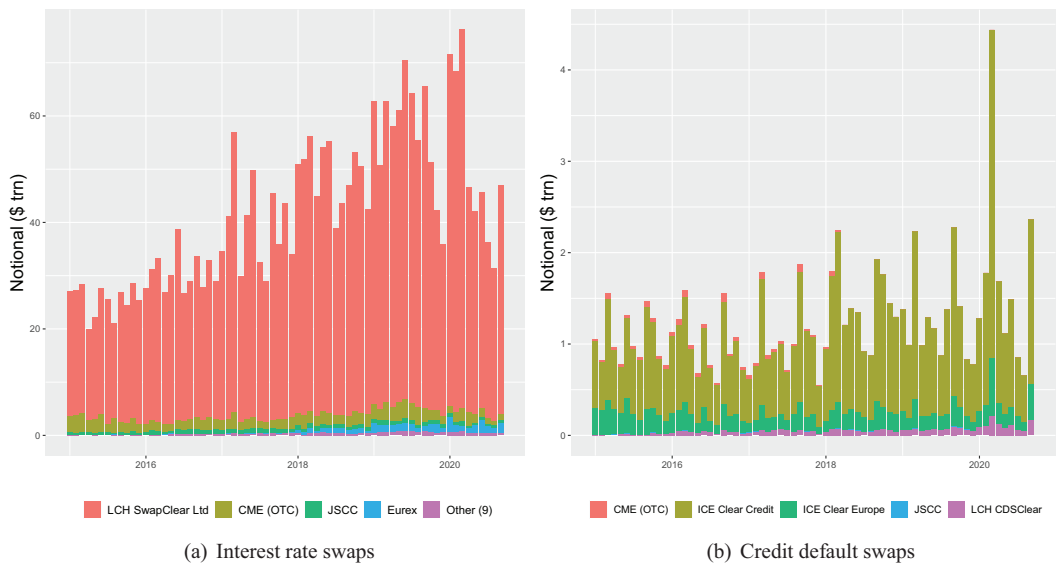


FIGURE 5 Notional amounts of derivatives cleared by market. (Note that the y-axes are on different scales due to the large volume of the IRS market.)

[Color figure can be viewed at [wileyonlinelibrary.com](https://onlinelibrary.wiley.com)]

Source: Clarus FT.

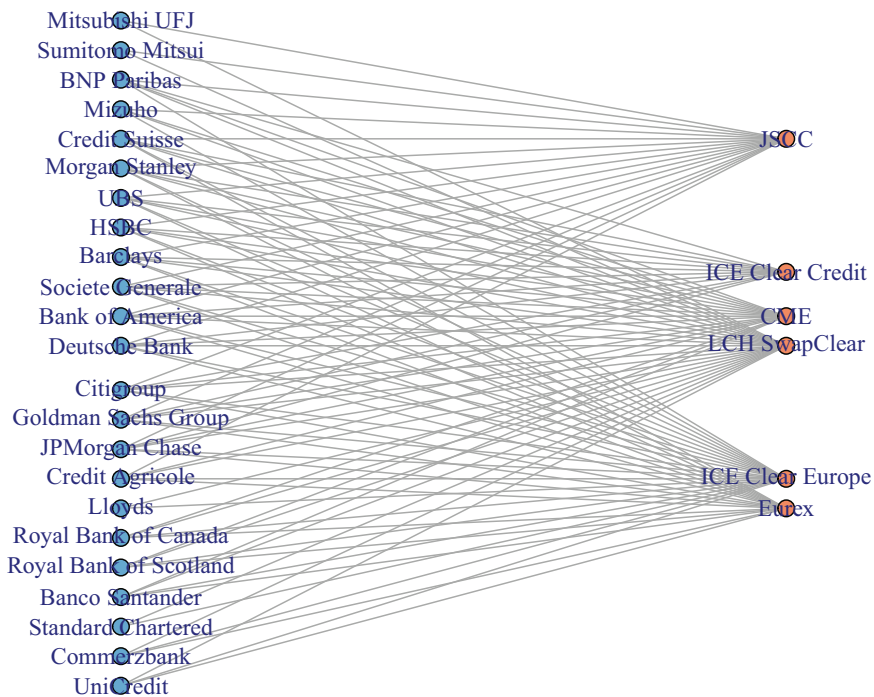
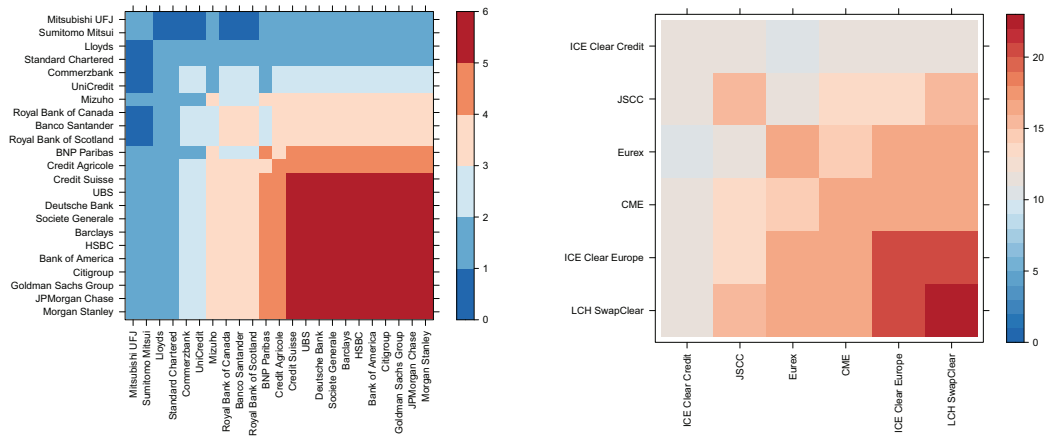


FIGURE 6 Bipartite network of clearing members and CCPs. [Color figure can be viewed at [wileyonlinelibrary.com](https://onlinelibrary.wiley.com)]



(a) Levelplot of $P^{members}$; each cell $P_{ij}^{members}$ shows the total number of CCPs at which both institutions i and j clear. (b) Levelplot of P^{CCPs} ; each cell P_{ij}^{CCPs} shows the total number of joint clearing members of CCPs i and j .

FIGURE 7 Graphical illustrations of $P^{members}$ (left) and P^{CCPs} (right). [Color figure can be viewed at wileyonlinelibrary.com]

clearing members means that they are joint clearing members in at least one CCP. An edge in the network of CCPs means that they share at least one clearing member.

First, we consider a one-mode projection that will create a network whose nodes are all the clearing members. The edges in the new network are undirected and weighted, where the weights represent the number of CCPs at which both clearing members clear. Formally, this is computed as follows. The original bipartite network consists of clearing members and CCPs. We consider the incidence matrix B for n_C groups (the CCPs) and n_M participants (the clearing members), which is given by $B \in \{0, 1\}^{n_C \times n_M}$, where

$$B_{ij} = \begin{cases} 1, & \text{if institution } j \text{ is a clearing member of CCP } i, \\ 0, & \text{otherwise.} \end{cases}$$

Then, for $i, j \in \{1, \dots, n_M\}$ and $k \in \{1, \dots, n_C\}$, it holds that $B_{ki}B_{kj} = 1$ if and only if both institutions i and j clear at CCP k . Therefore, the total number of CCPs where both i and j are clearing members is given by

$$P_{ij}^{members} = \sum_{k=1}^{n_C} B_{ki}B_{kj} = \sum_{k=1}^{n_C} B_{ik}^T B_{kj}.$$

In particular, $P^{members} = B^T B \in \{0, 1, \dots, n_C\}^{n_M \times n_M}$ and its diagonal element $P_{ii}^{members} = \sum_{k=1}^{n_C} B_{ki}B_{ki} = \sum_{k=1}^{n_C} B_{ki}$ represents the total number of CCPs where $i \in \{1, \dots, n_M\}$ is a clearing member.

Figure 7a presents a heatmap of $P^{members}$: roughly half of all institutions are clearing members of all six CCPs (red area).

The second one-mode projection creates a network that consists only of CCPs. Its edges are again undirected and weighted, with weights representing the number of shared clearing members. Formally, the total number of institutions that are clearing members at both CCPs i and j is

given by

$$P_{ij}^{\text{CCPs}} = \sum_{k=1}^{n_M} B_{ik} B_{jk} = \sum_{k=1}^{n_M} B_{ik} B_{kj}^{\top}.$$

In particular, $P^{\text{CCPs}} = BB^{\top} \in \{0, 1, \dots, n_M\}^{n_C \times n_C}$ and its diagonal element $P_{ii}^{\text{CCPs}} = \sum_{k=1}^{n_M} B_{ik}$ represents the total number of clearing members that CCP $i \in \{1, \dots, n_C\}$ has.

Figure 7 presents a heatmap of P^{CCPs} . There exists exactly one CCP, namely LCH, which has all 23 institutions considered here as its clearing members.

Both one-mode projections P^{members} and P^{CCPs} derived from our empirical data represent complete networks. This implies that losses from one CCP can in principle spill over to all other CCPs and losses of clearing members can in principle spill over to all other clearing members, if the corresponding liquidity buffers/IMs/default funds/and so forth are not large enough to stop the loss transmission.

5 | STRESS-TESTING CCPs

We will now show how our modeling framework can be used for stress-testing CCPs and discuss policy implications. CCPs run regular in-house stress tests to ensure that adequate resources are available to withstand a variety of stress scenarios. In addition, authorities conduct system-wide stress tests.

Our model and findings have important implications for CCP stress testing. The most notable feature of CCP stress-testing is the Cover-2 standard, used in practice both for single CCP and system stress-testing (ESMA, 2020). The European Securities and Markets Authority (ESMA) coordinates EU-wide stress-testing of CCPs and has used the Cover-2 standard. In particular, ESMA distinguishes between two different types: the ‘‘Cover-2 groups per CCP’’ and ‘‘EU-wide Cover-2 groups.’’ Under the first type, the top 2 clearing members for each CCP are assumed to default only for that individual CCP. Under the second type, the top 2 clearing members chosen to be in default are identified based on exposures across all CCPs and are assumed to default at all CCPs (see ESMA (2020, p. 20/21) for details). Importantly, stress tests do not consider second-round effects arising from joint clearing membership (ESMA, 2020).

A key contribution of our paper is to illustrate how accounting for higher-order effects arising from shared clearing membership can affect stress-testing results. Two key insights emerge: higher-order effects increase losses, and, when coupled with frictions such as default costs or severe VMGH, they can change the identity of the top two clearing members that cause the largest losses. To illustrate this point, we perform an extensive stress-testing exercise based on IRS data.

5.1 | Calibrating the model

To calibrate the model for our stress testing case study, we use data for end-2019, available from public disclosures and sourced from Clarus FT. As in Figure 6, we focus on clearing members that are large globally systemic banks.

We are able to match various model elements. In particular, our data contain information on the CCPs (total notional cleared, default funds δ_i , skin-in-the-game σ_i , aggregate IMs $\sum_{j=1}^{n_M} m_{ji}$

for all $i \in C$) and the clearing members (total notional cleared, which we denote by l_i). These data provide a good picture of the default waterfall of CCPs. Furthermore, we know the clearing members for each CCP.

There are, however, two key model quantities that we do not observe in the data: (i) the liquidity buffers of clearing members (b^M), and (ii) the network of payment obligations (\bar{p}^{R1}).²³ For clearing members' liquidity buffers, we simulate numbers such that preshock (i.e., before setting some liquidity buffers to zero) there are no fundamental defaults.

The estimation of the matrix of payment obligations is more involved. Appendix B provides details on the network reconstruction approach, we use to estimate the matrix \bar{p}^{R1} from available information. In a nutshell, we design a constrained optimization problem that takes into account the data we know (total notional cleared by CCPs and members and adjacency matrix of connections between them) and some assumptions that constrain the target matrix, such as CCPs having matched books and netting positions, and clearing members not trading bilaterally. From this constrained optimization, we obtain an estimate of the matrix of derivative positions (X_{ij}), and we set the matrix of VM payment obligations as a proportion ν to those ($\bar{p}^{R1} = \nu X_{ij}$, for some constant $\nu \geq 0$; in the simulation studies we present below, we chose $\nu = 0.01$).²⁴

5.2 | Case study and policy implications

For our stress testing exercise in the IRS market, we consider the default of all possible clearing member pairs by wiping out their liquidity buffers and computing the attendant total shortfall for each case. Figure 8 presents the results. The x -axis represents the different clearing member pairs shocked and the y -axis represents the total relative payment shortfalls.²⁵

We start by evaluating the shortfall based only on first-order effects (black line) and use it to sort the pairs as the benchmark. We then compute the corresponding shortfalls in equilibrium (i.e., accounting for higher order effects) and additionally consider fire sales of collateral (i.e., $\alpha > 0$), default frictions (i.e., $\gamma_i^{(1)} < 1$ and/or $\gamma_i^{(2)} < 1$ for some i) and combinations thereof. Throughout this case study, if we consider $\alpha > 0$, we set $\alpha = -\log(0.4)/\Delta_{\text{total}} \approx 3.89 \times 10^{-6}$, where again Δ_{total} represents total IMs available in the system. This implies, that if all available collateral was sold, then the price of the collateral would decrease from 1 to 0.4.

Accounting for higher-order effects indeed results in higher shortfalls (black vs. red lines in Figure 8). More interesting, however, is the fact that the red line is no longer monotonically decreasing. If we account for additional frictions ($\gamma_i^{(1)} < 1$ and or $\gamma_i^{(2)} < 1$ for some $i \in \mathcal{N}$) then this nonmonotonicity becomes even more evident (e.g., blue and purple lines). This implies that a pair that leads to high first-order losses need not rank equally high when considering higher-order effects (with or without frictions). The very large spike in Figure 8 indicates that there is

²³ Note that it is in principle possible to collect or estimate these data. However, this requires access to proprietary data that are typically only accessible to regulators (see, e.g., Paddrik et al. (2020)).

²⁴ This assumption is a shortcut taken for calibration in the absence of actual data on variation margin payment obligations. It should not be taken to imply that in reality, variation margin payment obligations are proportional to notional amounts. We do not put stock in the numbers we obtain being representative of how that matrix looks in reality, nor in our stress-testing exercise being a real-world stress test. Our goal in this simulation exercise is to obtain a matrix of variation margin payment obligations to illustrate the mechanisms in the model.

²⁵ Since there are $n_M = 23$ clearing members in our data, there are $\binom{n_M}{2} = 253$ ways to select two clearing members to be shocked.

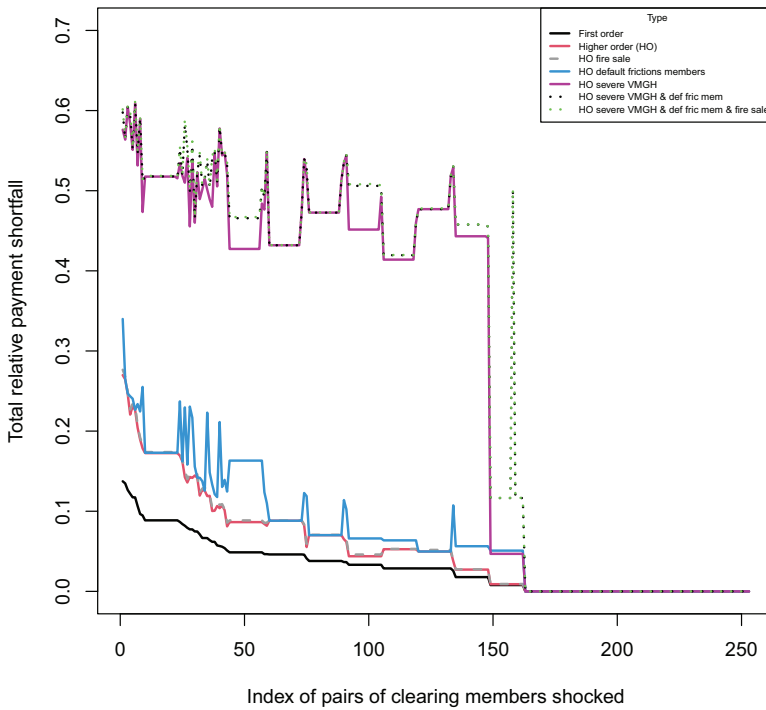


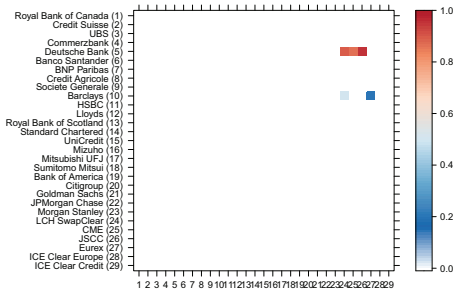
FIGURE 8 First- and higher-order total relative payment shortfalls when different pairs of clearing members are shocked for different parameter choices in Φ^{R1} . Relative payment shortfalls in the system can range between 0 and 1 (see Section 3). [Color figure can be viewed at wileyonlinelibrary.com]

one pair of clearing members that has very small losses when only considering first-order effects, but very high losses when accounting for higher-order effects and various frictions.

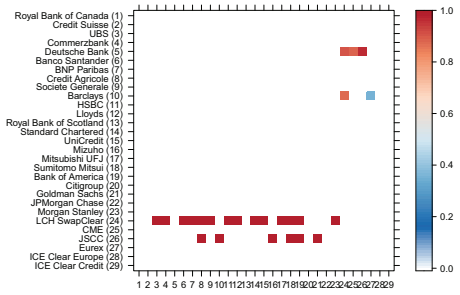
Default frictions are particularly powerful in affecting pair-specific shortfalls (and much more so than illiquid collateral). When considering default frictions of clearing members by setting $\gamma_i^{(1)} = \gamma_i^{(2)} = 0$ for all $i \in \mathcal{M}$ (blue line), shortfalls increase significantly, and the ordering of pairs leading to highest losses changes. When frictions are only associated with CCPs (purple line), that is, $\gamma_i^{(1)} = 1$ and $\gamma_i^{(2)} = 0$ for all $i \in \mathcal{C}$ (and $\gamma_i^{(1)} = \gamma_i^{(2)} = 1$ for all $i \in \mathcal{M}$), shortfalls increase even more and similarly the ordering of pairs leading to largest losses again varies considerably. In particular, the pair leading to the *largest* shortfalls is not the same as the pair that leads to the largest *first-order* shortfalls. When combining these two frictions for liquid (black dotted line) or illiquid collateral (green dotted line), shortfalls increase even further.

We next look at shortfalls for two specific pairs of clearing members. On the one side, the pair linked to the largest loss when looking at first-order effects; on the other side, we consider the pair linked to the largest losses when accounting for higher-order effects with illiquid collateral, and default frictions of clearing members and CCPs. We consider the parameters corresponding to Figure 8. In this example, there is no fundamental default before any pair is shocked. Under this scenario, the first pair (first-order effects only) is Deutsche Bank and Barclays, whereas the second pair is Deutsche Bank and the Royal Bank of Canada.

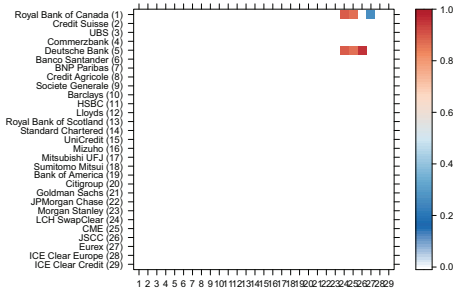
Figure 9 presents the results, with the first two panels focusing on the first pair and the last two panels focusing on the second pair. Figure 9a shows the first-order relative payment shortfall when Deutsche Bank and Barclays have their liquidity buffers set to 0, and Figure 9b shows the



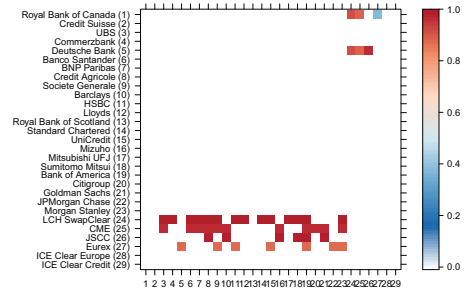
(a) First order relative payment shortfall for stress to Deutsche Bank and Barclays; total first order payment shortfall is 291,134 million USD.



(b) Higher order relative payment shortfall (with illiquid collateral and default frictions of both clearing members and CCPs) for stress to Deutsche Bank and Barclays; the total payment shortfall is 1,275,039 million USD.



(c) First order relative payment shortfall for stress to Deutsche Bank and the Royal Bank of Canada; total first order payment shortfall is 248,592 million USD.



(d) Higher order relative payment shortfall (with illiquid collateral and default frictions of both clearing members and CCPs) for stress to Deutsche Bank and the Royal Bank of Canada; total payment shortfall is 1,297,541 million USD.

FIGURE 9 First-order (left) and higher-order (right) relative payment shortfall when two different pairs of clearing members have their liquidity buffer set to 0. In the first row, Deutsche Bank and Barclays are selected to have 0 liquidity buffer, in the second row, Deutsche Bank and the Royal Bank of Canada are selected. The liquidity buffers are chosen such that there is no fundamental default prior to the stress-testing exercise. [Color figure can be viewed at wileyonlinelibrary.com]

corresponding higher-order relative payment shortfall that accounts for illiquid collateral, hard defaults of clearing members and severe VMGH, that is, $\alpha \approx 3.89 \times 10^{-6} > 0$, $\gamma_i^{(1)} = \gamma_i^{(2)} = 0$ for all $i \in \mathcal{M}$, and $\gamma_i^{(1)} = 1, \gamma_i^{(2)} = 0$ for all $i \in \mathcal{C}$. In this example, accounting for these higher-order effects increases the total shortfall from 291,134 (million USD) to 1,275,039 (million USD), that is, the shortfall is more than 4.4 times larger.

For the second pair, the picture that emerges is similar. Figure 9c shows the first-order relative payment shortfall when Deutsche Bank and the Royal Bank of Canada have their liquidity buffers set to 0, and Figure 9d shows the corresponding higher-order relative payment shortfall that accounts for the same frictions as before. Accounting for higher-order effects takes the total shortfall from 248,592 to 1,297,541 (million USD), that is, the shortfall is more than 5.2 times larger. In particular, four CCPs default under this scenario.

Taken together, these results illustrate that higher-order effects and frictions interact and affect the ordering of pairs causing the largest losses. Considering only first-order effects would yield Deutsche Bank and Barclays as the top pair, with a shortfall of 291,134 (million USD) (Figure 9a).

However, accounting for higher-order effects and frictions would deliver a considerably larger shortfall (1,297,541 million USD) by a different pair (Deutsche Bank and the Royal Bank of Canada, Figure 9d). To be sufficiently severe, stress testing should consider higher-order effects as well as potential market-related frictions.

6 | CONCLUSION

This paper underscores the important role that joint clearing members can have in loss transmission between several CCPs, especially in a context with realistic frictions. As such, it serves to highlight the need to incorporate these features into the current CCP stress testing practice. Furthermore, it also highlights the importance of stress testing CCPs simultaneously and not just in isolation.

As our case studies illustrate, in the presence of joint clearing members, it is even theoretically possible that a clearing member triggers the default of a CCP at which it does not clear. This can happen indirectly via fire sales of illiquid collateral, or directly via VMGH of the CCP at which the member clears, or a combination of both. Admittedly, situations like this would be rare, but nevertheless, they illustrate the importance of accounting for second- and higher-order interconnections between CCPs in their risk management.

It is important to bear in mind that our model is stylized and results are illustrative of the mechanisms we aim to highlight. Throughout we analyze how the effects of a clearing members' default play out mechanically through CCP's rulebooks, by incorporating key elements of the latter on an enhanced version of a canonical network contagion model. When interpreting results, it should be clear that we are not able to quantify the likelihood of any scenario leading to an actual CCP default.

That said, we are able to illustrate important issues regarding contagion in markets with multiple CCPs and joint clearing membership. In our case studies, we made a number of simplifying assumptions not required by our key results to go through, such as clearing members novating all their trades to CCPs, having no bilateral positions with other clearing members, or disregarding the links between clearing members and the clients they clear for. Even under these assumptions, which essentially remove several additional ways in which contagion can spread through the network of payment obligations, we still find strong contagion effects that can amplify losses considerably. Importantly, these contagion effects significantly change the ranking of clearing members, which cause the largest losses in case of default.

These results suggest that any Cover-2 standard that excludes network effects has the risk of being not conservative enough. One of the key lessons after the Great Financial Crisis was that stress scenarios need to be "sufficiently severe" (Basel Committee on Banking Supervision, 2018, Principle 4). Our paper provides evidence that accounting for network effects and joint clearing membership can be crucial to achieving this objective.

ACKNOWLEDGMENTS

The views expressed in this article are those of the authors and do not necessarily reflect those of the Bank for International Settlements (BIS). Parts of this research were carried out while Luitgard Veraart was a BIS Research Fellow at the Bank for International Settlements, whose hospitality and funding are gratefully acknowledged. We thank Marco Bardoscia, Rama Cont, Wenqian Huang, Alper Odabasioglu, Alexander Soreff, Nikola Tarashev, participants at the IMSI Workshop on Systemic Risk and Stress Testing, the UCL Financial Computing and Analytics Seminar,

the 11th World Congress of the Bachelier Finance Society, the 2022 SIAM Annual Meeting, the Stochastic Analysis and Mathematical Finance Seminar at the University of Oxford, the Bank of Canada conference “Networks in Modern Financial and Payments Systems,” the PSE-HEC-BdF workshop “Central clearing and market infrastructures: new challenges,” the 2023 LPFMI INET Workshop, the German Probability and Statistics Days 2023, the 2023 SIAM Conference on Financial Mathematics and Engineering, as well as seminar participants at the BIS and ESMA and the review team for helpful comments and suggestions.

CONFLICT OF INTEREST STATEMENT

The authors declare no conflicts of interest.

DATA AVAILABILITY STATEMENT

The data that support the findings of this study are available from Clarus Financial Technology. Restrictions apply to the availability of these data, which were used under license for this study.

ORCID

Luitgard Anna Maria Veraart  <https://orcid.org/0000-0003-1183-2227>

REFERENCES

- Amini, H., & Feinstein, Z. (2023). Optimal network compression. *European Journal of Operational Research*, 306, 1439–1455.
- Amini, H., Filipović, D., & Minca, A. (2015). *Systemic risk and central clearing counterparty design* [Swiss Finance Institute Research Paper no. 13-34]. Available at SSRN: <https://ssrn.com/abstract=2275376>
- Amini, H., Filipović, D., & Minca, A. (2016). Uniqueness of equilibrium in a payment system with liquidation costs. *Operations Research Letters*, 44, 1–5.
- Banerjee, T., & Feinstein, Z. (2019). Impact of contingent payments on systemic risk in financial networks. *Mathematics and Financial Economics*, 13, 617–636.
- Bardoscia, M., Ferrara, G., Vause, N., & Yoganayagam, M. (2019). Full payment algorithm. Available at SSRN: <https://ssrn.com/abstract=3344580>
- Basel Committee on Banking Supervision. (2018). *Stress testing principles*. <https://www.bis.org/bcbps/publ/d450.htm>
- BCBS-CPMI-FSB-IOSCO. (2018). *Analysis of central clearing interdependencies* (Technical Report 181). Basel Committee on Banking Supervision, Committee on Payments and Market Infrastructures, Financial Stability Board, International Organization of Securities Commissions.
- Biais, B., Heider, F., & Hoerova, M. (2016). Risk-sharing or risk-taking? Counterparty risk, incentives, and margins. *The Journal of Finance*, 71, 1669–1698.
- Bignon, V., & Vuillemeys, G. (2020). The failure of a clearinghouse: Empirical evidence. *Review of Finance*, 24, 99–128.
- Boissel, C., Derrien, F., Ors, E., & Thesmar, D. (2017). Systemic risk in clearing houses: Evidence from the European repo market. *Journal of Financial Economics*, 125, 511–536.
- Cifuentes, R., Shin, H. S., & Ferrucci, G. (2005). Liquidity risk and contagion. *Journal of the European Economic Association*, 3, 556–566.
- Cont, R. (2015). The end of the waterfall: Default resources of central counterparties. *Journal of Risk Management in Financial Institutions*, 8, 365–389.
- Cont, R. (2017). *Central clearing and risk transformation*. Financial Stability Review. Banque de France. No. 21.
- Cont, R., & Kokholm, T. (2014). Central clearing of OTC derivatives: Bilateral vs multilateral netting. *Statistics & Risk Modeling*, 31, 3–22.
- CPMI-IOSCO. (2018). *Framework for supervisory stress testing of central counterparties (CCPs)*. Committee on Payments and Market Infrastructures (CPMI), Board of the International Organization of Securities Commissions (IOSCO). www.bis.org

- CPMI-IOSCO. (2020). *Central counterparty default management auctions – issues for consideration*. Committee on Payments and Market Infrastructures (CPMI), Board of the International Organization of Securities Commissions (IOSCO). www.bis.org
- Csóka, P., & Herings, P. J.-J. (2018). Decentralized clearing in financial networks. *Management Science*, *64*, 4681–4699.
- Demange, G., & Piquard, T. (2021). *On the market structure of central counterparties in the EU*. Preprint. <https://halshs.archives-ouvertes.fr/halshs-03107812>
- Domanski, D., Gambacorta, L., & Picillo, C. (2015). Central clearing: Trends and current issues. *BIS Quarterly Review*.
- Duffie, D. (2014). *Resolution of failing central counterparties* [Research papers 3256]. Graduate School of Business, Stanford University.
- Duffie, D., & Zhu, H. (2011). Does a central clearing counterparty reduce counterparty risk? *Review of Asset Pricing Studies*, *1*, 74–95.
- D'Errico, M., & Roukny, T. (2021). Compressing over-the-counter markets. *Operations Research*, *69*, 1660–1679.
- Eisenberg, L., & Noe, T. H. (2001). Systemic risk in financial systems. *Management Science*, *47*, 236–249.
- Elsinger, H. (2011). *Financial networks, cross holdings, and limited liability* [Working paper 156]. Oesterreichische Nationalbank.
- ESMA. (2020). *3rd EU-wide stress test* (Report ESMA-151-3186). European Securities and Markets Authority (ESMA).
- ESRB. (2020). *Mitigating the procyclicality of margins and haircuts in derivatives markets and securities financing transactions* (Technical Report). European Systemic Risk Board.
- Faruqui, U., Huang, W., & Takáts, E. (2018). Clearing risks in OTC derivatives markets: The CCP-bank nexus. *BIS Quarterly Review*.
- Ferrara, G., Li, X., & Marszalec, D. (2020). Central counterparty auction design. *Journal of Financial Market Infrastructures*, *8*, 47–58.
- Gandy, A., & Veraart, L. A. M. (2017). A Bayesian methodology for systemic risk assessment in financial networks. *Management Science*, *63*, 4428–4446.
- Garratt, R., & Zimmerman, P. (2015). *Does central clearing reduce counterparty risk in realistic financial networks?* (Staff Reports) (pp. 1–18). Federal Reserve Bank of New York.
- Ghamami, S., Glasserman, P., & Young, H. P. (2022). Collateralized networks. *Management Science*, *68*, 2202–2225.
- Glasserman, P., Moallemi, C. C., & Yuan, K. (2015). Hidden illiquidity with multiple central counterparties. *Operations Research*, *64*, 1143–1158.
- Greenwood, R., Landier, A., & Thesmar, D. (2015). Vulnerable banks. *Journal of Financial Economics*, *115*, 471–485.
- Gregory, J. (2014). *Central counterparties: Mandatory central clearing and initial margin requirements for OTC derivatives*. Wiley Finance.
- Huang, W. (2019). *Central counterparty capitalization and misaligned incentives* [BIS working papers 767]. Bank for International Settlements.
- Huang, W., & Takats, E. (2020). *Model risk at central counterparties: Is skin-in-the-game a game changer?* [BIS working papers 866]. Bank for International Settlements.
- Huang, W., & Zhu, H. (2024). CCP auction design. *Journal of Economic Theory*, *217*, 105826.
- ISDA. (2013). *CCP loss allocation at the end of the waterfall* (Technical Report). International Swaps and Derivatives Association.
- Kusnetsov, M., & Veraart, L. A. M. (2019). Interbank clearing in financial networks with multiple maturities. *SIAM Journal on Financial Mathematics*, *10*, 37–67.
- Lopez, J. A. C., Harris, J. H., Hurlin, C., & Pérignon, C. (2017). Comargin. *Journal of Financial and Quantitative Analysis*, *52*, 2183–2215.
- Menkveld, A. J., & Vuillemeij, G. (2021). The economics of central clearing. *Annual Review of Financial Economics*, *13*, 153–178.
- Newman, M. E. J. (2010). *Networks – an introduction*. Oxford University Press.
- O'Kane, D. (2017). Optimising the multilateral netting of fungible OTC derivatives. *Quantitative Finance*, *17*, 1–12.
- Paddrik, M., Rajan, S., & Young, H. P. (2020). Contagion in derivatives markets. *Management Science*, *66*, 3603–3616.
- Paddrik, M., & Young, H. P. (2021). How safe are central counterparties in credit default swap markets? *Mathematics and Financial Economics*, *15*, 41–57.

Rogers, L. C. G., & Veraart, L. A. M. (2013). Failure and rescue in an interbank network. *Management Science*, 59, 882–898.

Schrimpf, A. (2015). Outstanding OTC derivatives positions dwindle as compression gains further traction. *BIS Quarterly Review*.

Tarski, A. (1955). A lattice theoretical fixed point theorem. *Pacific Journal of Mathematics*, 5, 285–309.

Veraart, L. A. M. (2022). When does portfolio compression reduce systemic risk? *Mathematical Finance*, 32, 727–778.

Veraart, L. A. M., & Zhang, Y. (2021). A macroprudential view on portfolio rebalancing and compression. Available at SSRN: <https://ssrn.com/abstract=3860262>

Wang, J. J., Capponi, A., & Zhang, H. (2022). A theory of collateral requirements for central counterparties. *Management Science*, 68, 6993–7017.

How to cite this article: Veraart, L. A. M., & Aldasoro, I. (2024). Systemic risk in markets with multiple central counterparties. *Mathematical Finance*, 1–49. <https://doi.org/10.1111/mafi.12446>

APPENDIX A: EXISTENCE RESULTS AND PROOFS

Lemma A.1 (Properties of Φ^{RI}). *Let $\Phi^{RI} : [0, 1] \times [0, \bar{p}^{RI}] \rightarrow [0, 1] \times [0, \bar{p}^{RI}]$ be the function defined in Equation (1), then Φ^{RI} is order-preserving, that is, for all $\tilde{\pi}, \pi \in [0, 1]$ with $\tilde{\pi} \leq \pi$ and for all $\tilde{p}, p \in [0, \bar{p}^{RI}]$ with $\tilde{p}_{ij} \leq p_{ij}$ for all $i, j \in \mathcal{N}$, it holds that*

$$\begin{aligned} \Phi_1^{RI}(\tilde{\pi}, \tilde{p}) &\leq \Phi_1^{RI}(\pi, p), \\ \Phi_{2,(i,j)}^{RI}(\tilde{\pi}, \tilde{p}) &\leq \Phi_{2,(i,j)}^{RI}(\pi, p) \quad \forall i, j \in \mathcal{N}. \end{aligned}$$

Proof of Lemma A.1. Let $\tilde{\pi}, \pi \in [0, 1]$ with $\tilde{\pi} \leq \pi$ and let $\tilde{p}, p \in [0, \bar{p}^{RI}]$ with $\tilde{p}_{ij} \leq p_{ij}$ for all $i, j \in \mathcal{N}$.

We show that Φ_1^{RI} is order-preserving. The total assets satisfy

$$A_i(\tilde{p}) = b_i + \sum_{k=1}^N \tilde{p}_{ki} \leq b_i + \sum_{k=1}^N p_{ki} = A_i(p).$$

This implies that all nodes that default under p also default under \tilde{p} , in particular

$$D(p) \subseteq D(\tilde{p}), \tag{A.1}$$

since for $i \in D(p)$, it holds that $\bar{p}_i^{RI} > A_i(p) \geq A_i(\tilde{p})$, and hence $i \in D(\tilde{p})$.

Next, we need to show that the number of shares of collateral sold satisfies

$$\Delta_{ij}(\tilde{\pi}, \tilde{p}) \geq \Delta_{ij}(\pi, p) \quad \forall i, j \in \mathcal{N}. \tag{A.2}$$

Once this has been shown, we immediately obtain that

$$\Delta(\tilde{\pi}, \tilde{p}) = \sum_{i=1}^N \sum_{j=1}^N \Delta_{ij}(\tilde{\pi}, \tilde{p}) \geq \sum_{i=1}^N \sum_{j=1}^N \Delta_{ij}(\pi, p) = \Delta(\pi, p),$$

and hence

$$\Phi_1^{\text{R1}}(\tilde{\pi}, \tilde{p}) = \exp(-\alpha\Delta(\tilde{\pi}, \tilde{p})) \leq \exp(-\alpha\Delta(\pi, p)) = \Phi_1^{\text{R1}}(\pi, p),$$

since $\alpha \geq 0$.

We now prove Equation (A.2). Let $i, j \in \mathcal{N}$.

- First, let $i \in D(p)$. By Equation (A.1), $i \in D(\tilde{p})$. We distinguish between three cases:

Case 1: Let $\tilde{\pi} > 0$, then, $\Delta_{ij}(\tilde{\pi}, \tilde{p}) = \min \left\{ m_{ij}, \frac{\tilde{p}_{ij}^{\text{R1}}}{\tilde{\pi}} \right\}$ and $\Delta_{ij}(\pi, p) = \min \left\{ m_{ij}, \frac{\tilde{p}_{ij}^{\text{R1}}}{\pi} \right\}$. Since

$0 < \tilde{\pi} \leq \pi$, it holds that $\frac{\tilde{p}_{ij}^{\text{R1}}}{\tilde{\pi}} \geq \frac{\tilde{p}_{ij}^{\text{R1}}}{\pi}$, which implies that

$$\Delta_{ij}(\tilde{\pi}, \tilde{p}) = \min \left\{ m_{ij}, \frac{\tilde{p}_{ij}^{\text{R1}}}{\tilde{\pi}} \right\} \geq \min \left\{ m_{ij}, \frac{\tilde{p}_{ij}^{\text{R1}}}{\pi} \right\} = \Delta_{ij}(\pi, p).$$

Case 2: Let $\tilde{\pi} = \pi = 0$, then if $\tilde{p}_{ij}^{\text{R1}} > 0$, it holds that $\Delta_{ij}(\tilde{\pi}, \tilde{p}) = m_{ij} = \Delta_{ij}(\pi, p)$. If $\tilde{p}_{ij}^{\text{R1}} = 0$, then $\Delta_{ij}(\tilde{\pi}, \tilde{p}) = 0 = \Delta_{ij}(\pi, p)$.

Case 3: Let $0 = \tilde{\pi} < \pi$, then if $\tilde{p}_{ij}^{\text{R1}} > 0$, it holds that $\Delta_{ij}(\tilde{\pi}, \tilde{p}) = m_{ij} \geq \min \left\{ m_{ij}, \frac{\tilde{p}_{ij}^{\text{R1}}}{\pi} \right\} = \Delta_{ij}(\pi, p)$. If $\tilde{p}_{ij}^{\text{R1}} = 0$, then $\Delta_{ij}(\tilde{\pi}, \tilde{p}) = 0 = \min \left\{ m_{ij}, \frac{\tilde{p}_{ij}^{\text{R1}}}{\pi} \right\} = \Delta_{ij}(\pi, p)$.

- Second, let $i \in \mathcal{N} \setminus D(p)$. Then, $\Delta_{ij}(\pi, p) = 0 \leq \Delta_{ij}(\tilde{\pi}, \tilde{p})$. Hence, Equation (A.2) holds.

Next, we show that Φ_2^{R1} is order-preserving. Let $i, j \in \mathcal{N}$. We distinguish between two cases.

Case 1: Let $i \in \mathcal{N} \setminus D(p)$. Then,

$$\Phi_{2,(ij)}^{\text{R1}}(\pi, p) = \tilde{p}_{ij}^{\text{R1}} \geq \Phi_{2,(ij)}^{\text{R1}}(\tilde{\pi}, \tilde{p}).$$

Case 2: Let $i \in D(p)$. Then, $i \in D(\tilde{p})$. Then,

$$\begin{aligned} \Phi_{2,(ij)}^{\text{R1}}(\tilde{\pi}, \tilde{p}) &= \min \left\{ \tilde{p}_{ij}^{\text{R1}}, \tilde{\pi} m_{ij} + a_{ij}^{\text{R1}}(\tilde{\pi}) \left(\gamma_i^{(1)} b_i + \gamma_i^{(2)} \sum_{k=1}^N \tilde{p}_{ki} \right) \right\}, \\ \Phi_{2,(ij)}^{\text{R1}}(\pi, p) &= \min \left\{ \tilde{p}_{ij}^{\text{R1}}, \pi m_{ij} + a_{ij}^{\text{R1}}(\pi) \left(\gamma_i^{(1)} b_i + \gamma_i^{(2)} \sum_{k=1}^N p_{ki} \right) \right\}. \end{aligned}$$

We distinguish between two cases.

First, let $\Phi_{2,(ij)}^{\text{R1}}(\pi, p) = \tilde{p}_{ij}^{\text{R1}}$, then $\Phi_{2,(ij)}^{\text{R1}}(\pi, p) = \tilde{p}_{ij}^{\text{R1}} \geq \Phi_{2,(ij)}^{\text{R1}}(\tilde{\pi}, \tilde{p})$.

Second, let

$$\tilde{p}_{ij}^{\text{R1}} > \Phi_{2,(ij)}^{\text{R1}}(\pi, p) = \pi m_{ij} + a_{ij}^{\text{R1}}(\pi) \left(\gamma_i^{(1)} b_i + \gamma_i^{(2)} \sum_{k=1}^N p_{ki} \right). \tag{A.3}$$

We show that

$$\bar{p}_{ij}^{R1} > \Phi_{2,(ij)}^{R1}(\tilde{\pi}, \tilde{p}) = \tilde{\pi}m_{ij} + a_{ij}^{R1}(\tilde{\pi}) \left(\gamma_i^{(1)}b_i + \gamma_i^{(2)} \sum_{k=1}^N \tilde{p}_{ki} \right). \tag{A.4}$$

Rearranging Equation (A.3) gives $\bar{p}_{ij}^{R1} - \pi m_{ij} > a_{ij}^{R1}(\pi) \left(\gamma_i^{(1)}b_i + \gamma_i^{(2)} \sum_{k=1}^N p_{ki} \right) \geq 0$ and hence

$$0 < \frac{\bar{p}_{ij}^{R1} - \pi m_{ij}}{\sum_{k=1}^N \max\{0, \bar{p}_{ik}^{R1} - \pi m_{ik}\}} = a_{ij}^{R1}(\pi),$$

which implies that

$$\begin{aligned} \bar{p}_{ij}^{R1} - \pi m_{ij} &> a_{ij}^{R1}(\pi) \left(\gamma_i^{(1)}b_i + \gamma_i^{(2)} \sum_{k=1}^N p_{ki} \right) = \frac{\bar{p}_{ij}^{R1} - \pi m_{ij}}{\sum_{k=1}^N \max\{0, \bar{p}_{ik}^{R1} - \pi m_{ik}\}} \left(\gamma_i^{(1)}b_i + \gamma_i^{(2)} \sum_{k=1}^N p_{ki} \right), \\ \Leftrightarrow 1 &> \frac{\left(\gamma_i^{(1)}b_i + \gamma_i^{(2)} \sum_{k=1}^N p_{ki} \right)}{\sum_{k=1}^N \max\{0, \bar{p}_{ik}^{R1} - \pi m_{ik}\}}. \end{aligned} \tag{A.5}$$

It also holds that $a_{ij}^{R1}(\tilde{\pi}) > 0$. We prove this by contradiction. Assume that $a_{ij}^{R1}(\tilde{\pi}) = 0$. This implies that $\bar{p}_{ij}^{R1} \leq \tilde{\pi}m_{ij}$. But since $0 = a_{ij}^{R1}(\tilde{\pi}) < a_{ij}^{R1}(\pi)$, we obtain

$$\tilde{\pi}m_{ij} + a_{ij}^{R1}(\tilde{\pi}) \left(\gamma_i^{(1)}b_i + \gamma_i^{(2)} \sum_{k=1}^N \tilde{p}_{ki} \right) \leq \pi m_{ij} + a_{ij}^{R1}(\pi) \left(\gamma_i^{(1)}b_i + \gamma_i^{(2)} \sum_{k=1}^N p_{ki} \right) = \Phi_{2,(ij)}^{R1}(\pi, p) < \bar{p}_{ij}^{R1},$$

which is a contradiction to $\bar{p}_{ij}^{R1} \leq \tilde{\pi}m_{ij}$. Hence, $a_{ij}^{R1}(\tilde{\pi}) > 0$.

From $a_{ij}^{R1}(\tilde{\pi}) > 0$, it follows directly that

$$\sum_{k=1}^N \max\{0, \bar{p}_{ik}^{R1} - \tilde{\pi}m_{ik}\} > 0 \text{ and } \bar{p}_{ij}^{R1} - \tilde{\pi}m_{ij} > 0. \tag{A.6}$$

Then,

$$\begin{aligned} \tilde{\pi}m_{ij} + a_{ij}^{R1}(\tilde{\pi}) \left(\gamma_i^{(1)}b_i + \gamma_i^{(2)} \sum_{k=1}^N \tilde{p}_{ki} \right) &= \tilde{\pi}m_{ij} + \frac{\max\{0, \bar{p}_{ij}^{R1} - \tilde{\pi}m_{ij}\}}{\sum_{k=1}^N \max\{0, \bar{p}_{ik}^{R1} - \tilde{\pi}m_{ik}\}} \left(\gamma_i^{(1)}b_i + \gamma_i^{(2)} \sum_{k=1}^N \tilde{p}_{ki} \right) \\ &\leq \tilde{\pi}m_{ij} + \frac{\max\{0, \bar{p}_{ij}^{R1} - \tilde{\pi}m_{ij}\}}{\sum_{k=1}^N \max\{0, \bar{p}_{ik}^{R1} - \pi m_{ik}\}} \left(\gamma_i^{(1)}b_i + \gamma_i^{(2)} \sum_{k=1}^N p_{ki} \right) < \tilde{\pi}m_{ij} + \max\{0, \bar{p}_{ij}^{R1} - \tilde{\pi}m_{ij}\} = \bar{p}_{ij}^{R1}, \end{aligned} \tag{A.7}$$

where the last inequality follows from Equation (A.5). Observe that Equation (A.3) implies that indeed $\sum_{k=1}^N \max\{0, \bar{p}_{ik}^{R1} - \pi m_{ik}\} > 0$. Hence, Equation (A.4) holds.

It remains to show that

$$\Phi_{2,(ij)}^{R1}(\tilde{\pi}, \tilde{p}) = \tilde{\pi}m_{ij} + a_{ij}^{R1}(\tilde{\pi}) \left(\gamma_i^{(1)}b_i + \gamma_i^{(2)} \sum_{k=1}^N \tilde{p}_{ki} \right)$$

$$\leq \pi m_{ij} + a_{ij}^{\text{R1}}(\pi) \left(\gamma_i^{(1)} b_i + \gamma_i^{(2)} \sum_{k=1}^N p_{ki} \right) = \Phi_{2,(ij)}^{\text{R1}}(\pi, p).$$

It is clear that $\Phi_{2,(ij)}^{\text{R1}}$ is order-preserving in the argument p . So we only need to show that it is also order-preserving in π . If $m_{ij} = 0$, then it follows directly that $a_{ij}^{\text{R1}}(\tilde{\pi}) \leq a_{ij}^{\text{R1}}(\pi)$ and hence $\Phi_{2,(ij)}^{\text{R1}}(\tilde{\pi}, \bar{p}) \leq \Phi_{2,(ij)}^{\text{R1}}(\pi, p)$. If $m_{ij} > 0$, we define a function $f_{ij}(\cdot; \hat{p}) : [\tilde{\pi}, \pi] \rightarrow [0, \bar{p}_{ij}^{\text{R1}}]$ by

$$f_{ij}(\hat{\pi}; \hat{p}) = \hat{\pi} m_{ij} + a_{ij}^{\text{R1}}(\hat{\pi}) \underbrace{\left(\gamma_i^{(1)} b_i + \gamma_i^{(2)} \sum_{k=1}^N \hat{p}_{ki} \right)}_{=A_i(\hat{p}; \gamma_i^{(1)}, \gamma_i^{(2)})} = \hat{\pi} m_{ij} + a_{ij}^{\text{R1}}(\hat{\pi}) A_i \left(\hat{p}; \gamma_i^{(1)}, \gamma_i^{(2)} \right),$$

where $\hat{p} \in [\bar{p}, p]$. In particular, $f_{ij}(\hat{\pi}; \hat{p}) = \Phi_{2,(ij)}^{\text{R1}}(\hat{\pi}, \hat{p})$ under the given constraints on the parameters.

Furthermore, since $a^{\text{R1}}(\tilde{\pi}) > 0$ and $a^{\text{R1}}(\pi) > 0$, we obtain for all $\hat{\pi} \in [\tilde{\pi}, \pi]$ that $\tilde{\pi} m_{ij} \leq \hat{\pi} m_{ij} \leq \pi m_{ij} < \bar{p}_{ij}^{\text{R1}}$ and hence $a_{ij}^{\text{R1}}(\hat{\pi}) > 0$.

From Equations (A.3) and (A.4), it follows directly that $A_i(p; \gamma_i^{(1)}, \gamma_i^{(2)}) < \sum_{k=1}^N \max\{0, \bar{p}_{ik}^{\text{R1}} - \pi m_{ik}\}$ and $A_i(\bar{p}; \gamma_i^{(1)}, \gamma_i^{(2)}) < \sum_{k=1}^N \max\{0, \bar{p}_{ik}^{\text{R1}} - \tilde{\pi} m_{ik}\}$. Hence, for all $\hat{p} \in [\bar{p}, p]$, we obtain

$$\begin{aligned} A_i \left(\hat{p}; \gamma_i^{(1)}, \gamma_i^{(2)} \right) &\leq A_i \left(\bar{p}; \gamma_i^{(1)}, \gamma_i^{(2)} \right) \leq A_i \left(p; \gamma_i^{(1)}, \gamma_i^{(2)} \right) < \sum_{k=1}^N \max \{0, \bar{p}_{ik}^{\text{R1}} - \pi m_{ik}\} \\ &\leq \sum_{k=1}^N \max \{0, \bar{p}_{ik}^{\text{R1}} - \hat{\pi} m_{ik}\} \leq \sum_{k=1}^N \max \{0, \bar{p}_{ik}^{\text{R1}} - \tilde{\pi} m_{ik}\}. \end{aligned} \tag{A.8}$$

The function f_{ij} is continuous and piecewise differentiable.²⁶ Similarly to the argument used in Ghamami et al. (2022, Proof of Lemma A.1), we can consider the derivative of f_{ij} , and obtain

$$\begin{aligned} \frac{\partial f_{ij}(\hat{\pi}; \hat{p})}{\partial \hat{\pi}} &= m_{ij} + \frac{\partial a_{ij}^{\text{R1}}(\hat{\pi})}{\partial \hat{\pi}} A_i \left(\hat{p}; \gamma_i^{(1)}, \gamma_i^{(2)} \right), \\ \frac{\partial a_{ij}^{\text{R1}}(\hat{\pi})}{\partial \hat{\pi}} &= \frac{\left(\sum_{k=1}^N \max \{0, \bar{p}_{ik}^{\text{R1}} - \hat{\pi} m_{ik}\} \right) (-m_{ij}) + \left(\bar{p}_{ij}^{\text{R1}} - \hat{\pi} m_{ij} \right)^+ \sum_{k=1}^N m_{ik} \mathbb{1}_{\{ \bar{p}_{ik}^{\text{R1}} > \hat{\pi} m_{ik} \}}}{\left(\sum_{k=1}^N \max \{0, \bar{p}_{ik}^{\text{R1}} - \hat{\pi} m_{ik}\} \right)^2}, \end{aligned}$$

and hence,

$$\frac{\partial f_{ij}(\hat{\pi}; \hat{p})}{\partial \hat{\pi}} = m_{ij} \left(1 - \frac{A_i(\hat{p}; \gamma_i^{(1)}, \gamma_i^{(2)})}{\sum_{k=1}^N \max \{0, \bar{p}_{ik}^{\text{R1}} - \hat{\pi} m_{ik}\}} \right) + \frac{\left(\bar{p}_{ij}^{\text{R1}} - \hat{\pi} m_{ij} \right)^+ \sum_{k=1}^N m_{ik} \mathbb{1}_{\{ \bar{p}_{ik}^{\text{R1}} > \hat{\pi} m_{ik} \}}}{\left(\sum_{k=1}^N \max \{0, \bar{p}_{ik}^{\text{R1}} - \hat{\pi} m_{ik}\} \right)^2} A_i \left(\hat{p}; \gamma_i^{(1)}, \gamma_i^{(2)} \right).$$

²⁶ The only points where f_{ij} is not differentiable are points $\bar{p}_{ik}^{\text{R1}}/m_{ik} \in [\tilde{\pi}, \pi]$ with $m_{ik} > 0, k \in \mathcal{N}$.

The first term of the derivative satisfies

$$1 - \frac{A_i \left(\hat{p}; \gamma_i^{(1)}, \gamma_i^{(2)} \right)}{\sum_{k=1}^N \max \{ 0, \bar{p}_{ik}^{R1} - \hat{\pi} m_{ik} \}} \geq 0,$$

because of Equation (A.8). Furthermore, it is clear that the second term of the derivative is non-negative. Hence, the derivative is non-negative. Together with the continuity of f_{ij} , this implies that f_{ij} is order-preserving on $[\bar{\pi}, \pi]$ and hence $\Phi_{2,(ij)}^{R1}(\bar{\pi}, \bar{p}) \leq \Phi_{2,(ij)}^{R1}(\pi, p)$. \square

Theorem A.2 (Existence of a least and greatest price-payment equilibrium in Round 1). *Let $\Phi^{R1} : [0, 1] \times [0, \bar{p}^{R1}] \rightarrow [0, 1] \times [0, \bar{p}^{R1}]$ be the function defined in Equation (1).*

1. *The set of fixed points of Φ^{R1} is a complete lattice. In particular, Φ^{R1} admits a greatest and a least fixed point.*
2. *Let $(\pi^{(0)}, p^{(0)}) = (1, \bar{p}^{R1})$ and define recursively for $k \in \mathbb{N}_0$*

$$(\pi^{(k+1)}, p^{(k+1)}) = \Phi^{R1}(\pi^{(k)}, p^{(k)}).$$

Then,

- (a) *$(\pi^{(k)}, p^{(k)})_{k \in \mathbb{N}_0}$ is a monotonically nonincreasing sequence, that is, $\pi^{(k+1)} \leq \pi^{(k)}$ and $p_{ij}^{(k+1)} \leq p_{ij}^{(k)}$ for all $i, j \in \mathcal{N}$ and for all $k \in \mathbb{N}_0$.*
- (b) *The limit $\lim_{k \rightarrow \infty} (\pi^{(k)}, p^{(k)})$ exists and is the greatest fixed point of Φ^{R1} .*

Proof of Theorem A.2.

1. We will prove the statement using Tarski’s fixed point theorem (Tarski, 1955). First, $[0, 1] \times [0, \bar{p}^{R1}]$ is a complete lattice with respect to the component-wise ordering. Second, it follows directly from the definition of Φ^{R1} in Equation (1) that indeed $\Phi^{R1} : [0, 1] \times [0, \bar{p}^{R1}] \rightarrow [0, 1] \times [0, \bar{p}^{R1}]$. Third, Φ^{R1} is an order-preserving function by Lemma A.1. By Tarski’s fixed point theorem, the set of fixed points of Φ^{R1} is a complete lattice and hence a least and greatest fixed point exist.
2. Next, we show that the greatest fixed point can be obtained by fixed point iteration.
 - (a) We prove that $\pi^{(k+1)} \leq \pi^{(k)}$ and $p_{ij}^{(k+1)} \leq p_{ij}^{(k)}$ for all $i, j \in \mathcal{N}$ and for all $k \in \mathbb{N}_0$ by induction.

For $k = 0$, it follows directly from the definition of Φ^{R1} in Equation (1) that $\pi^{(1)} = \Phi_1^{R1}(\pi^{(0)}, p^{(0)}) = \exp(-\alpha \Delta(\pi^{(0)}, p^{(0)})) \leq 1 = \pi^{(0)}$ and $p_{ij}^{(1)} = \Phi_{2,(ij)}^{R1}(\pi^{(0)}, p^{(0)}) \leq \bar{p}_{ij}^{R1} = p_{ij}^{(0)}$ for all $i, j \in \mathcal{N}$.

Our induction hypothesis is that $\pi^{(k+1)} \leq \pi^{(k)}$ and $p_{ij}^{(k+1)} \leq p_{ij}^{(k)}$ for all $i, j \in \mathcal{N}$ and for a $k \in \mathbb{N}_0$.

Then, by the definition of the sequence

$$(\pi^{(k+2)}, p^{(k+2)}) = \Phi^{R1}(\pi^{(k+1)}, p^{(k+1)}) \leq \Phi^{R1}(\pi^{(k)}, p^{(k)}) = (\pi^{(k+1)}, p^{(k+1)}),$$

where the inequality follows from the induction hypothesis and the fact that Φ^{R1} is order-preserving by Lemma A.1. Hence, this completes the induction step.

It follows directly from the definition of Φ^{R1} that it is bounded from below by $(0, 0)$ (where the first 0 is one-dimensional and the second zero is the $N \times N$ zero matrix). Hence, there exists a monotone limit $(\hat{\pi}, \hat{p}) = \lim_{k \rightarrow \infty} (\pi^{(k)}, p^{(k)})$. This limit is a fixed point of Φ^{R1} , since

$$\Phi^{R1}(\hat{\pi}, \hat{p}) = \Phi^{R1}\left(\lim_{k \rightarrow \infty} (\pi^{(k)}, p^{(k)})\right) = \lim_{k \rightarrow \infty} \Phi^{R1}(\pi^{(k)}, p^{(k)}) = \lim_{k \rightarrow \infty} (\pi^{(k+1)}, p^{(k+1)}) = (\hat{\pi}, \hat{p}),$$

where the second equality follows from the right-continuity of Φ^{R1} . It remains to show that $(\hat{\pi}, \hat{p}) = (\pi^{*,R1}, p^{*,R1})$, that is, that it is the greatest fixed point of Φ^{R1} .

We show by induction that $(\pi^{(k)}, p^{(k)}) \geq (\pi^{*,R1}, p^{*,R1})$ for all $k \in \mathbb{N}_0$. It is clear that $(\pi^{(0)}, p^{(0)}) = (1, \bar{p}^{R1}) \geq (\pi^{*,R1}, p^{*,R1})$. Suppose $(\pi^{(k)}, p^{(k)}) \geq (\pi^{*,R1}, p^{*,R1})$ for a $k \in \mathbb{N}_0$. Then,

$$(\pi^{(k+1)}, p^{(k+1)}) = \Phi^{R1}(\pi^{(k)}, p^{(k)}) \geq \Phi^{R1}(\pi^{*,R1}, p^{*,R1}) = (\pi^{*,R1}, p^{*,R1}),$$

where the inequality follows from the induction hypothesis and the fact that Φ^{R1} is order-preserving. The last equality holds because $(\pi^{*,R1}, p^{*,R1})$ is a fixed point of Φ^{R1} .

Hence,

$$(\hat{\pi}, \hat{p}) = \lim_{k \rightarrow \infty} (\pi^{(k)}, p^{(k)}) \geq (\pi^{*,R1}, p^{*,R1})$$

and since $(\hat{\pi}, \hat{p}) = \Phi^{R1}(\hat{\pi}, \hat{p})$, we obtain that $(\hat{\pi}, \hat{p}) = (\pi^{*,R1}, p^{*,R1})$. □

Corollary A.3. *It holds that $F \subseteq D(p^{*,R1})$.*

Proof of Corollary A.3. From Theorem A.2, $F = D(p^{(0)})$. Since, $(p^{(k)})_{k \in \mathbb{N}_0}$ is monotonically nonincreasing, it holds that for all $k \in \mathbb{N}$

$$D(p^{(k)}) = \left\{ i \in \mathcal{N} \mid b_i + \sum_{\nu=1}^N p_{\nu i}^{(k)} < \bar{p}_i^{R1} \right\} \subseteq \left\{ i \in \mathcal{N} \mid b_i + \sum_{\nu=1}^N p_{\nu i}^{(k+1)} < \bar{p}_i^{R1} \right\} = D(p^{(k+1)}).$$

Hence, in particular $F = D(p^{(0)}) \subseteq D(p^{*,R1})$. □

Remark A.4. The existence of a greatest and least fixed point for the second round of clearing was proved in Ghamami et al. (2022). In particular, $[0, \pi^{*,R1}] \times [0, \bar{p}^{R2}]$ is a complete lattice with respect to the component-wise ordering and Φ^{R2} is order-preserving. The greatest fixed point of Φ^{R2} , therefore, exists by Tarski's fixed point theorem.

Additionally, since Φ^{R2} is also right-continuous, one can show using the same type of arguments as for Φ^{R1} , that the greatest fixed point $(\pi^{*,R2}, p^{*,R2})$ of Φ^{R2} can be obtained by setting $(\pi^{(0)}, p^{(0)}) = (\pi^{*,R1}, \bar{p}^{R2})$ and then defining recursively for $k \in \mathbb{N}_0$

$$(\pi^{(k+1)}, p^{(k+1)}) = \Phi^{R2}(\pi^{(k)}, p^{(k)}),$$

which is a nonincreasing sequence that is bounded from below by $(0, 0)$ (as it was the case for Φ^{R1}). In particular, $(\pi^{*,R2}, p^{*,R2}) = \lim_{k \rightarrow \infty} \Phi^{R2}(\pi^{(k)}, p^{(k)})$, that is, it converges to the greatest fixed point.

APPENDIX B: DATA DESCRIPTION AND NETWORK RECONSTRUCTION FOR THE CASE STUDIES

Our case studies rely on data from CCP public disclosures, which we source from Clarus FT. These data provide a substantial amount of information that can be directly used to calibrate our model. For each CCP $i \in \{1, \dots, n_C\}$, we know its clearing members and we observe the total notional cleared (denoted by a_i), the default fund (δ_i), the CCP’s capital (i.e., skin-in-the-game σ_i), and the aggregate IMs ($\sum_{j=1}^{n_M} m_{ji}$). This is enough to have a well-rounded picture of CCP’s waterfalls, which we illustrate in Figure B.1 for the CCPs in our sample (aggregated over both IRS and CDS data). As the figure shows, the bulk of loss-absorbing resources are given by IMs and the default fund, whereas skin-in-the-game is thin to a level that is almost imperceptible in the graphs. In addition, we also obtain, for each clearing member $i \in \{1, \dots, n_M\}$, the total notional cleared by market (denoted by l_i).

There are, however, some important model objects that we do not observe, most notably the network of VM payment obligations (\bar{p}^{R1}). Accordingly, we need to estimate it based on observable data. In the following, we describe how we estimate this network.

We start with a matrix of notional positions, $X \in [0, \infty)^{N \times N}$, where X_{ij} is the total liability from i to j arising from a derivative contract. We assume that the first n_M rows and columns correspond to the clearing members, and the last n_C rows and columns correspond to CCPs. Hence,

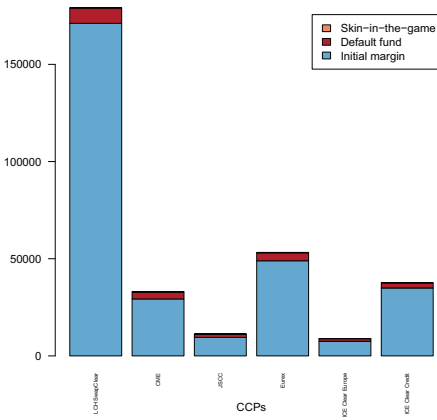
$$X = \left(\begin{array}{ccc|ccc} X_{1,1} & \dots & X_{1,n_M} & X_{1,(n_M+1)} & X_{1,(n_M+2)} & \dots & X_{1,(n_M+n_C)} \\ \dots & \dots & \dots & \dots & \dots & \dots & \dots \\ X_{n_M,1} & \dots & X_{n_M,n_M} & X_{n_M,(n_M+1)} & X_{n_M,(n_M+2)} & \dots & X_{n_M,(n_M+n_C)} \\ \hline X_{(n_M+1),1} & \dots & X_{(n_M+1),n_M} & X_{(n_M+1),(n_M+1)} & X_{(n_M+1),(n_M+2)} & \dots & X_{(n_M+1),(n_M+n_C)} \\ \dots & \dots & \dots & \dots & \dots & \dots & \dots \\ X_{(n_M+n_C),1} & \dots & X_{(n_M+n_C),n_M} & X_{(n_M+n_C),(n_M+1)} & X_{(n_M+n_C),(n_M+2)} & \dots & X_{(n_M+n_C),(n_M+n_C)} \end{array} \right)$$

$$= \left(\begin{array}{c|c} A & B \\ \hline C & D \end{array} \right),$$

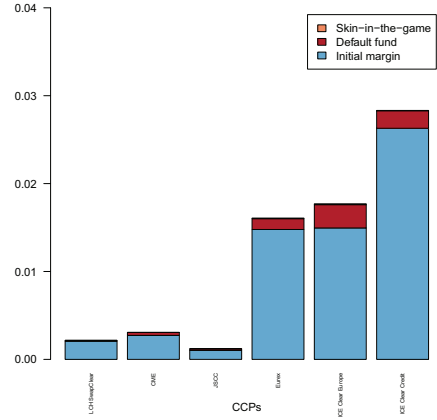
where $A \in [0, \infty)^{n_M \times n_M}$, $B \in [0, \infty)^{n_M \times n_C}$, $C \in [0, \infty)^{n_C \times n_M}$, $D \in [0, \infty)^{n_C \times n_C}$.

In our empirical analyses, we assume that clearing members do not trade bilaterally. This implies that the upper left $n_M \times n_M$ -dimensional submatrix A is the zero matrix. Similarly, since the CCPs do not have any trading relationships with other CCPs, the lower right $n_C \times n_C$ -dimensional submatrix D is also the zero matrix. Hence, we need to estimate the following two submatrices:

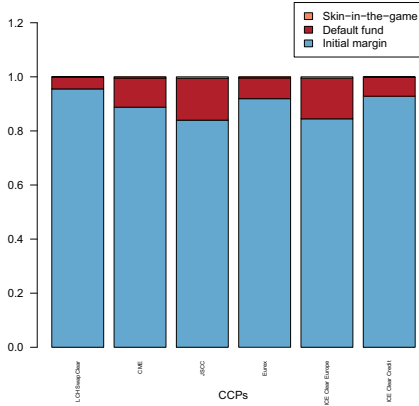
$$B = \left(\begin{array}{ccc} X_{1,(n_M+1)} & \dots & X_{1,(n_M+n_C)} \\ \dots & \dots & \dots \\ X_{n_M,(n_M+1)} & \dots & X_{n_M,(n_M+n_C)} \end{array} \right),$$



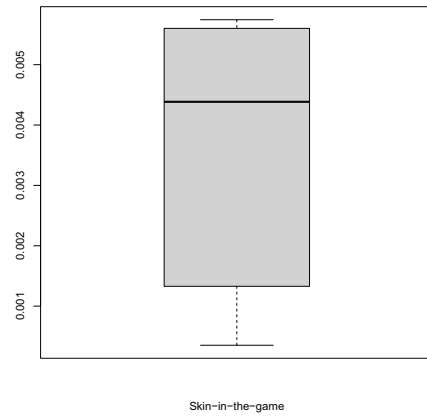
(a) Default waterfall for each CCP (in million USD).



(b) Default waterfall normalised by the total exposure cleared for each CCP.



(c) Default waterfall normalised by the total size of the default waterfall for each CCP.



(d) Boxplot of Skin-in-the-game normalised by the total size of the default waterfall for each CCP.

FIGURE B.1 Default waterfall for the six CCPs (original (top left), normalized by total exposure (top right) and by the size of the default waterfall (bottom left)), and boxplot of the normalized skin-in-the game (bottom right). [Color figure can be viewed at wileyonlinelibrary.com]

$$C = \begin{pmatrix} X_{(n_M+1),1} & \dots & X_{(n_M+1),n_M} \\ \dots & \dots & \dots \\ X_{(n_M+n_C),1} & \dots & X_{(n_M+n_C),n_M} \end{pmatrix}.$$

Since positions at CCPs are netted, we assume that there are no index pairs $i, j \in \mathcal{N}$ such that both $X_{ij} > 0$ and $X_{ji} > 0$ for $i, j \in \mathcal{N}$. This implies that there are no index pairs for which both $B_{ij} > 0$ and $C_{ji} > 0$, where $i \in \{1, \dots, n_M\}$ and $j \in \{1, \dots, n_C\}$.

Hence, we can estimate the two matrices B, C simultaneously, by estimating the matrix $Y \in \mathbb{R}^{n_M \times n_C}$, where $Y = B - C^T$. In particular, Y can take positive and negative entries. Fix $i \in \{1, \dots, n_M\}$ and $j \in \{1, \dots, n_C\}$. First, if $Y_{i,j} \geq 0$, we set $B_{ij} = X_{i,(n_M+j)} = Y_{i,j}$, which means that clearing member i has an obligation to CCP j and we set $C_{j,i} = X_{(n_M+j),i} = 0$ (i.e., no obligation

from CCP j to clearing member i). Second, if $Y_{ij} < 0$, then we set $B_{ij} = X_{i,(n_M+j)} = 0$, that is, clearing member i does not have any obligations to CCP j , and we set $C_{j,i} = X_{(n_M+j),i} = |Y_{ij}|$, that is, the CCP j has an obligation to clearing member i .

We have the following information about Y . From public disclosures, we know the clearing members of each CCP. This means that we know the adjacency matrix that corresponds to Y , which we denote by $A^{\text{observed}} \in \{0, 1\}^{n_M \times n_C}$. In particular,

$$A_{ij}^{\text{observed}} = \begin{cases} 1, & \text{if } i \text{ is a clearing member of } j, \\ 0, & \text{else.} \end{cases}$$

Furthermore, as mentioned above, for each clearing member $i \in \{1, \dots, n_M\}$, we know the total notional amount that it clears (l_i). In turn, for each CCP $j \in \{1, \dots, n_C\}$, we know the total notional that it clears, denoted by a_j . Moreover, we also know that each CCP has a matched book, as that is the essence of their business model. These considerations together give rise to the following mathematical constraints on matrix Y :

$$\begin{aligned} \sum_{j=1}^{n_C} |Y_{ij} A_{ij}^{\text{observed}}| &= l_i \quad \forall i \in \{1, \dots, n_M\} \quad (\text{total notional cleared by clearing member}) \\ \sum_{i=1}^{n_M} |Y_{ij} A_{ij}^{\text{observed}}| &= a_j \quad \forall j \in \{1, \dots, n_C\} \quad (\text{total notional cleared by CCP}) \\ \sum_{i=1}^{n_M} Y_{ij} A_{ij}^{\text{observed}} &= 0 \quad \forall j \in \{1, \dots, n_C\} \quad (\text{matched book of CCP}). \end{aligned} \tag{B.1}$$

Given these additional constraints, we cannot use standard methods available to reconstruct financial networks from the observed row and column sums, see, for example, Gandy and Veraart (2017) and the references therein.

To obtain a matrix Y , we solve an optimization problem that penalizes deviations from the constraints formulated in Equation (B.1). We consider the following objective function $f : R^{n_M \times n_C} \rightarrow \mathbb{R}$, where

$$f(y) = \sum_{i=1}^{n_M} \left(l_i - \sum_{j=1}^{n_C} |Y_{ij} A_{ij}^{\text{observed}}| \right)^2 + \sum_{j=1}^{n_C} \left(a_j - \sum_{i=1}^{n_M} |Y_{ij} A_{ij}^{\text{observed}}| \right)^2 + P \sum_{j=1}^{n_C} \left(\sum_{i=1}^{n_M} Y_{ij} A_{ij}^{\text{observed}} \right)^2,$$

where $P > 0$ is a constant that we include to put an additional penalty weight on the term that captures how well the CCPs' books are matched. Then, we consider the following optimization problem:

$$\begin{aligned} \min_{Y \in R^{n_M \times n_C}} & f(Y) \\ \text{subject to} & \text{Adj}(Y) = A^{\text{observed}}, \end{aligned}$$

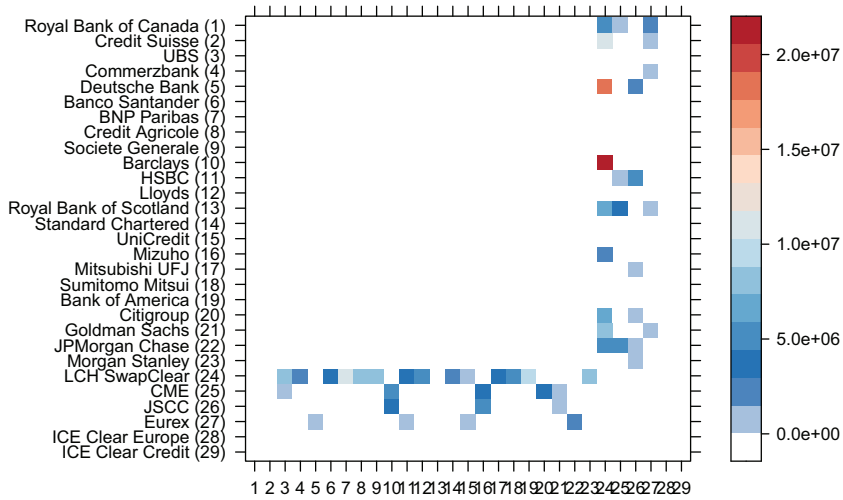


FIGURE B.2 Reconstructed network of derivative positions for interest rate swaps (in million USD). [Color figure can be viewed at wileyonlinelibrary.com]

where $Adj(Y)_{ij} = 1$ if $Y_{ij} > 0$ and 0 otherwise, hence it computes the adjacency matrix that corresponds to Y .²⁷

When solving this optimization problem for our data for the IRS and CDS markets, we obtain in both cases matrices in which CCPs have indeed (essentially) matched books, and the deviations from the observed row and column sums are very small²⁸. After having obtained the matrix Y , we can use it to compute the matrix X of notional positions as described before. Figure B.2 shows the reconstructed matrix of IRS notional amounts.

Finally, we then assume that the VM payments due from derivative positions are proportional to the original estimated position, that is, if the derivative position is X_{ij} , then we set $\bar{p}_{ij}^{RI} = \nu X_{ij}$ for some constant $\nu \geq 0$.

The final quantities we need are the liquidity buffers of the clearing members, that is, b_i , where $i \in \mathcal{M}$. Since we do not have this information, we simulate numbers such that preshock (i.e., before setting some liquidity buffers to 0) there are no fundamental defaults.

APPENDIX C: CLEARING WITH PECKING ORDER

In this appendix, we develop a clearing mechanism in which clearing members that default do not pay the CCPs pro rata (as assumed in our benchmark model) but according to a pecking order, and compare the results. We use ideas developed in Elsinger (2011) for clearing networks with different seniorities of debt. We characterize the pecking order in terms of a matrix $\Omega \in \{0, 1, \dots, n_C\}^{n_M \times n_C}$, where Ω_{ij} represents the rank of CCP j in clearing member i 's pecking order. If $\Omega_{ij} = 1$, this means that CCP j is paid first by clearing member i , and payments to other CCPs are only made if assets are left after the payments to j are made. If $\Omega_{ij} = 0$, then this means that clearing member i does not have any payment obligations to CCP j . In the following, we assume that each clearing

²⁷ In fact, we only need to find those Y_{ij} for which $A_{ij}^{observed} = 1$. Hence, the number of unknown parameters can be reduced from $n_M \cdot n_C$ to $\sum_{i=1}^{n_M} \sum_{j=1}^{n_C} A_{ij}^{(Y)}$.

²⁸ For the IRS data, the objective function is 1.061781e-11 and for the CDS data, the objective function is 1.967258e-15.

member has a strict ranking of CCPs to which it makes payments, so no two CCPs are considered of equal seniority in a clearing member's pecking order.²⁹

Our mathematical model does not depend on which criteria are used by the clearing members to decide on their pecking order. For our case studies, we assume that the pecking order is obtained by considering the size of the payment obligations, that is, a clearing member ranks the CCP to which it has the highest payment obligations first in the pecking order and then pays other CCPs according to decreasing nominal amounts of payments due. As before, we assume that CCPs still pay their clearing members pro rata and not according to a pecking order.

C.1 | First round of clearing with pecking order

In the following, we assume that $\bar{p}_i^{R1} > 0$ for all $i \in \mathcal{C}$, that is, all CCPs have strictly positive payment obligations. Since CCPs have matched books, this means that we do not have redundant CCPs in the model. To simplify notation, we assume that $\mathcal{M} = \{1, \dots, n_M\}$ and $\mathcal{C} = \{n_M + 1, \dots, n_M + n_C\}$, that is, the first n_M indices correspond to the clearing members and the remaining indices to the CCPs.

We can characterize a price-payment equilibrium as a suitable fixed point. We consider a function $\Phi^{R1, \text{pecking}} : [0, 1] \times [0, \bar{p}^{R1}] \rightarrow [0, 1] \times [0, \bar{p}^{R1}]$, and are interested in a fixed point $(\pi^{*,R1, \text{pecking}}, p^{*,R1, \text{pecking}})$ such that

$$(\pi^{*,R1, \text{pecking}}, p^{*,R1, \text{pecking}}) = \Phi^{R1, \text{pecking}}(\pi^{*,R1, \text{pecking}}, p^{*,R1, \text{pecking}}),$$

where $\Phi^{R1, \text{pecking}}$ is defined as follows.

$$\begin{aligned} \Phi_1^{R1}(\pi, p) &= \exp(-\alpha \Delta(\pi, p)), \\ \Phi_{2,(ij)}^{R1, \text{pecking}}(p) &= \begin{cases} \min \left\{ \bar{p}_{ij}^{R1}, \frac{\bar{p}_{ij}^{R1}}{\sum_{k=1}^N \bar{p}_{ik}^{R1}} \left(\gamma_i^{(1)} b_i + \gamma_i^{(2)} \sum_{k=1}^N p_{ki} \right) \right\}, & \text{if } i \in \mathcal{C} \cap \mathcal{D}(p), \\ \min \left\{ \bar{p}_{ij}^{R1}, \pi m_{ij} + \left(\gamma_i^{(1)} b_i + \gamma_i^{(2)} \sum_{k=1}^N p_{ki} - W_{ij}(\pi) \right)^+ \right\}, & \text{if } i \in \mathcal{M} \cap \mathcal{D}(p), \\ \bar{p}_{ij}^{R1}, & \text{if } i \in \mathcal{N} \setminus \mathcal{D}(p), \end{cases} \end{aligned} \tag{C.1}$$

where as before $\mathcal{D}(p) = \{i \in \mathcal{N} \mid A_i(p) < \bar{p}_i^{R1}\}$, specifies the nodes in default in a system with payments $p \in [0, \bar{p}^{R1}]$, and again $A_i(p) = b_i + \sum_{k=1}^N p_{ki}$ denotes the available assets of node $i \in \mathcal{N}$.

Furthermore,

$$W_{ij}(\pi) = \sum_{k=1}^{n_C} \left(\bar{p}_{i,n_M+k}^{R1} - \pi m_{i,n_M+k} \right)^+ \mathbb{1}_{\{\Omega_{ik} < \Omega_{ij}\}},$$

²⁹ Our model is related to that of Elsinger (2011), who adapt the Eisenberg and Noe (2001) framework to a setting with different seniorities of debt. In contrast to Elsinger (2011), our framework includes (possibly illiquid) collateral and bankruptcy costs and is, therefore, more general. We have formulated our model for a strict pecking order, but this assumption can be relaxed and one can consider a situation in which more than one CCP can have the same rank in the pecking order. This would lead to a slightly different definition of $\Phi^{R1, \text{pecking}}$.

that is, $W_{ij}(\pi)$ are the payment obligations (that remain after seizing the IMs for these positions at a current price of $\pi \in [0, 1]$ per share) of clearing member i to the CCPs that are before CCP j in the pecking order. Again $\Delta(\pi, p)$ models the total number of shares of collateral sold in Round 1 and it is defined exactly as in Section 2.

When comparing $\Phi^{R1, \text{pecking}}$ in Equation (C.1) to Φ^{R1} in Equation (1), the only difference is for $i \in \mathcal{M} \cap \mathcal{D}(p)$, that is, for defaulting clearing members. In Equation (1), defaulting clearing members paid the CCPs pro rata, that is, they distributed their available assets according to the proportions $a_{ij}^{R1}(\pi) = \frac{\max\{0, \bar{p}_{ij}^{R1} - \pi m_{ij}\}}{\sum_{k=1}^N \max\{0, \bar{p}_{ik}^{R1} - \pi m_{ik}\}}$. When there is a pecking order, this is no longer the case. A defaulting clearing member first uses all its assets to pay the CCP ranked first, then uses the remaining assets to pay the CCP ranked second, and so on. This is captured by the second branch of $\Phi^{R1, \text{pecking}}$ in Equation (C.1). The term $(\gamma_i^{(1)} b_i + \gamma_i^{(2)} \sum_{k=1}^N p_{ki} - W_{ij}(\pi))^+$ captures the resources that clearing member i can use to pay the CCP j with pecking order rank Ω_{ij} on top of the IMs.

Lemma C.1 (Properties of $\Phi^{R1, \text{pecking}}$). *Let $\Phi^{R1, \text{pecking}} : [0, 1] \times [0, \bar{p}^{R1}] \rightarrow [0, 1] \times [0, \bar{p}^{R1}]$ be the function defined in Equation (C.1), then $\Phi^{R1, \text{pecking}}$ is order-preserving.*

Proof of Lemma C.1. Let $\tilde{\pi}, \pi \in [0, 1]$ with $\tilde{\pi} \leq \pi$ and let $\tilde{p}, p \in [0, \bar{p}^{R1}]$ with $\tilde{p}_{ij} \leq p_{ij}$ for all $i, j \in \mathcal{N}$.

Since $\Phi_1^{R1, \text{pecking}}$ is identical to Φ_1^{R1} , we know from the proof of Theorem A.2 that $\Phi_1^{R1, \text{pecking}}$ is order-preserving.

Next, we show that $\Phi_2^{R1, \text{pecking}}$ is order-preserving. Based on the same arguments as in the proof of Theorem A.2, it holds that

$$D(p) \subseteq D(\tilde{p}). \tag{C.2}$$

Next, we show that Φ_2^{R1} is order-preserving. Let $i, j \in \mathcal{N}$. We distinguish between three cases.

Case 1: Let $i \in \mathcal{N} \setminus D(p)$. Then,

$$\Phi_{2,(ij)}^{R1, \text{pecking}}(\pi, p) = \bar{p}_{ij}^{R1} \geq \Phi_{2,(ij)}^{R1, \text{pecking}}(\tilde{\pi}, \tilde{p}).$$

Case 2: Let $i \in C \cap D(p)$. Then, $i \in C \cap D(\tilde{p})$. Then,

$$\begin{aligned} \Phi_{2,(ij)}^{R1, \text{pecking}}(\tilde{\pi}, \tilde{p}) &= \min \left\{ \bar{p}_{ij}^{R1}, \frac{\bar{p}_{ij}^{R1}}{\sum_{k=1}^N \bar{p}_{ik}^{R1}} \left(\gamma_i^{(1)} b_i + \gamma_i^{(2)} \sum_{k=1}^N \tilde{p}_{ki} \right) \right\}, \\ \Phi_{2,(ij)}^{R1, \text{pecking}}(\pi, p) &= \min \left\{ \bar{p}_{ij}^{R1}, \frac{\bar{p}_{ij}^{R1}}{\sum_{k=1}^N \bar{p}_{ik}^{R1}} \left(\gamma_i^{(1)} b_i + \gamma_i^{(2)} \sum_{k=1}^N p_{ki} \right) \right\}. \end{aligned}$$

We distinguish between two cases. First, let $\Phi_{2,(ij)}^{R1, \text{pecking}}(\pi, p) = \bar{p}_{ij}^{R1}$, then

$$\Phi_{2,(ij)}^{R1}(\pi, p) = \bar{p}_{ij}^{R1} \geq \Phi_{2,(ij)}^{R1, \text{pecking}}(\tilde{\pi}, \tilde{p}).$$

Second, let

$$\bar{p}_{ij}^{R1} > \Phi_{2,(ij)}^{R1, \text{pecking}}(\pi, p). \tag{C.3}$$

Then,

$$\begin{aligned} \bar{p}_{ij}^{R1} > \Phi_{2,(ij)}^{R1, \text{pecking}}(\pi, p) &= \frac{\bar{p}_{ij}^{R1}}{\sum_{k=1}^N \bar{p}_{ik}^{R1}} \left(\gamma_i^{(1)} b_i + \gamma_i^{(2)} \sum_{k=1}^N p_{ki} \right) \geq \frac{\bar{p}_{ij}^{R1}}{\sum_{k=1}^N \bar{p}_{ik}^{R1}} \left(\gamma_i^{(1)} b_i + \gamma_i^{(2)} \sum_{k=1}^N \tilde{p}_{ki} \right) \\ &= \Phi_{2,(ij)}^{R1, \text{pecking}}(\tilde{\pi}, \tilde{p}), \end{aligned}$$

where the last equality follows from assumption (C.3).

Case 3: Let $i \in \mathcal{M} \cap D(p)$. Then, $i \in \mathcal{M} \cap D(\tilde{p})$. Then,

$$\begin{aligned} \Phi_{2,(ij)}^{R1, \text{pecking}}(\tilde{\pi}, \tilde{p}) &= \min \left\{ \bar{p}_{ij}^{R1}, \tilde{\pi} m_{ij} + \left(\gamma_i^{(1)} b_i + \gamma_i^{(2)} \sum_{k=1}^N \tilde{p}_{ki} - W_{ij}(\tilde{\pi}) \right)^+ \right\}, \\ \Phi_{2,(ij)}^{R1, \text{pecking}}(\pi, p) &= \min \left\{ \bar{p}_{ij}^{R1}, \pi m_{ij} + \left(\gamma_i^{(1)} b_i + \gamma_i^{(2)} \sum_{k=1}^N p_{ki} - W_{ij}(\pi) \right)^+ \right\}. \end{aligned}$$

Again, we distinguish between two cases. First, let $\Phi_{2,(ij)}^{R1, \text{pecking}}(\pi, p) = \bar{p}_{ij}^{R1}$, then

$$\Phi_{2,(ij)}^{R1}(\pi, p) = \bar{p}_{ij}^{R1} \geq \Phi_{2,(ij)}^{R1, \text{pecking}}(\tilde{\pi}, \tilde{p}).$$

Second, let

$$\bar{p}_{ij}^{R1} > \Phi_{2,(ij)}^{R1, \text{pecking}}(\pi, p). \tag{C.4}$$

It follows directly from the definition of W_{ij} , that $W_{ij}(\pi) \leq W_{ij}(\tilde{\pi})$ and hence $-W_{ij}(\pi) \geq -W_{ij}(\tilde{\pi})$. Hence,

$$\bar{p}_{ij}^{R1} > \Phi_{2,(ij)}^{R1, \text{pecking}}(\pi, p) = \min \left\{ \bar{p}_{ij}^{R1}, \pi m_{ij} + \left(\gamma_i^{(1)} b_i + \gamma_i^{(2)} \sum_{k=1}^N p_{ki} - W_{ij}(\pi) \right)^+ \right\}$$

$$\begin{aligned} &\geq \min \left\{ \tilde{p}_{ij}^{R1}, \tilde{\pi} m_{ij} + \left(\gamma_i^{(1)} b_i + \gamma_i^{(2)} \sum_{k=1}^N \tilde{p}_{ki} - W_{ij}(\tilde{\pi}) \right)^+ \right\} \\ &= \Phi_{2,(ij)}^{R1, \text{pecking}}(\tilde{\pi}, \tilde{p}), \end{aligned}$$

where the last equality follows from assumption (C.4). Hence, indeed $\Phi^{R1, \text{pecking}}$ is order-preserving. \square

Theorem C.2 (Existence of a least and greatest price-payment equilibrium in Round 1 in the setting with a pecking order). *Let $\Phi^{R1, \text{pecking}} : [0, 1] \times [0, \bar{p}^{R1}] \rightarrow [0, 1] \times [0, \bar{p}^{R1}]$ be the function defined in Equation (C.1).*

1. *The set of fixed points of $\Phi^{R1, \text{pecking}}$ is a complete lattice. In particular, $\Phi^{R1, \text{pecking}}$ admits a greatest and a least fixed point.*
2. *Let $(\pi^{(0)}, p^{(0)}) = (1, \bar{p}^{R1})$ and define recursively for $k \in \mathbb{N}_0$*

$$(\pi^{(k+1)}, p^{(k+1)}) = \Phi^{R1, \text{pecking}}(\pi^{(k)}, p^{(k)}).$$

Then,

- (a) *$(\pi^{(k)}, p^{(k)})_{k \in \mathbb{N}_0}$ is a monotonically nonincreasing sequence, that is, $\pi^{(k+1)} \leq \pi^{(k)}$ and $p_{ij}^{(k+1)} \leq p_{ij}^{(k)}$ for all $i, j \in \mathcal{N}$ and for all $k \in \mathbb{N}_0$.*
- (b) *The limit $\lim_{k \rightarrow \infty} (\pi^{(k)}, p^{(k)})$ exists and is the greatest fixed point of $\Phi^{R1, \text{pecking}}$.*

Proof of Theorem C.2.

1. We will prove the statement using Tarski’s fixed point theorem (Tarski, 1955). First, $[0, 1] \times [0, \bar{p}^{R1}]$ is a complete lattice with respect to the component-wise ordering. Second, it follows directly from the definition of $\Phi^{R1, \text{pecking}}$ in Equation (1) that indeed $\Phi^{R1, \text{pecking}} : [0, 1] \times [0, \bar{p}^{R1}] \rightarrow [0, 1] \times [0, \bar{p}^{R1}]$. Third, $\Phi^{R1, \text{pecking}}$ is an order-preserving function by Lemma C.1. By Tarski’s fixed point theorem, the set of fixed points of $\Phi^{R1, \text{pecking}}$ is a complete lattice and hence a least and greatest fixed point exist.
2. This statement can be proved along the lines of the proof of Theorem A.2. We provide the details below.
 - (a) We prove that $\pi^{(k+1)} \leq \pi^{(k)}$ and $p_{ij}^{(k+1)} \leq p_{ij}^{(k)}$ for all $i, j \in \mathcal{N}$ and for all $k \in \mathbb{N}_0$ by induction.

For $k = 0$, it follows directly from the definition of $\Phi^{R1, \text{pecking}}$ in Equation (C.1) that $\pi^{(1)} = \Phi_1^{R1, \text{pecking}}(\pi^{(0)}, p^{(0)}) = \exp(-\alpha \Delta(\pi^{(0)}, p^{(0)})) \leq 1 = \pi^{(0)}$ and $p_{ij}^{(1)} = \Phi_{2,(ij)}^{R1, \text{pecking}}(\pi^{(0)}, p^{(0)}) \leq \bar{p}_{ij}^{R1} = p_{ij}^{(0)}$ for all $i, j \in \mathcal{N}$.

Our induction hypothesis is that $\pi^{(k+1)} \leq \pi^{(k)}$ and $p_{ij}^{(k+1)} \leq p_{ij}^{(k)}$ for all $i, j \in \mathcal{N}$ and for a $k \in \mathbb{N}_0$.

Then, by the definition of the sequence

$$(\pi^{(k+2)}, p^{(k+2)}) = \Phi^{R1, \text{pecking}}(\pi^{(k+1)}, p^{(k+1)}) \leq \Phi^{R1, \text{pecking}}(\pi^{(k)}, p^{(k)}) = (\pi^{(k+1)}, p^{(k+1)}),$$

where the inequality follows from the induction hypothesis and the fact that $\Phi^{R1, \text{pecking}}$ is order-preserving by Lemma C.1. Hence, this completes the induction step.

It follows directly from the definition of $\Phi^{R1, \text{pecking}}$ that it is bounded from below by $(0, 0)$ (where the first 0 is one-dimensional and the second zero is the $N \times N$ zero matrix). Hence, there exists a monotone limit $(\hat{\pi}, \hat{p}) = \lim_{k \rightarrow \infty} (\pi^{(k)}, p^{(k)})$. This limit is a fixed point of $\Phi^{R1, \text{pecking}}$, since

$$\begin{aligned} \Phi^{R1, \text{pecking}}(\hat{\pi}, \hat{p}) &= \Phi^{R1, \text{pecking}}(\lim_{k \rightarrow \infty} (\pi^{(k)}, p^{(k)})) = \lim_{k \rightarrow \infty} \Phi^{R1, \text{pecking}}(\pi^{(k)}, p^{(k)}) \\ &= \lim_{k \rightarrow \infty} (\pi^{(k+1)}, p^{(k+1)}) = (\hat{\pi}, \hat{p}), \end{aligned}$$

where the second equality follows from the right-continuity of $\Phi^{R1, \text{pecking}}$. It remains to show that $(\hat{\pi}, \hat{p}) = (\pi^{*,R1, \text{pecking}}, p^{*,R1, \text{pecking}})$, that is, that it is the greatest fixed point of $\Phi^{R1, \text{pecking}}$.

We show by induction that $(\pi^{(k)}, p^{(k)}) \geq (\pi^{*,R1, \text{pecking}}, p^{*,R1, \text{pecking}})$ for all $k \in \mathbb{N}_0$. It is clear that $(\pi^{(0)}, p^{(0)}) = (1, \bar{p}^{R1}) \geq (\pi^{*,R1, \text{pecking}}, p^{*,R1, \text{pecking}})$. Suppose

$(\pi^{(k)}, p^{(k)}) \geq (\pi^{*,R1, \text{pecking}}, p^{*,R1, \text{pecking}})$ for a $k \in \mathbb{N}_0$. Then,

$$\begin{aligned} (\pi^{(k+1)}, p^{(k+1)}) &= \Phi^{R1, \text{pecking}}(\pi^{(k)}, p^{(k)}) \\ &\geq \Phi^{R1, \text{pecking}}(\pi^{*,R1, \text{pecking}}, p^{*,R1, \text{pecking}}) = (\pi^{*,R1, \text{pecking}}, p^{*,R1, \text{pecking}}), \end{aligned}$$

where the inequality follows from the induction hypothesis and the fact that $\Phi^{R1, \text{pecking}}$ is order-preserving. The last equality holds because $(\pi^{*,R1, \text{pecking}}, p^{*,R1, \text{pecking}})$ is a fixed point of $\Phi^{R1, \text{pecking}}$.

Hence,

$$(\hat{\pi}, \hat{p}) = \lim_{k \rightarrow \infty} (\pi^{(k)}, p^{(k)}) \geq (\pi^{*,R1, \text{pecking}}, p^{*,R1, \text{pecking}})$$

and since $(\hat{\pi}, \hat{p}) = \Phi^{R1, \text{pecking}}(\hat{\pi}, \hat{p})$, we obtain $(\hat{\pi}, \hat{p}) = (\pi^{*,R1, \text{pecking}}, p^{*,R1, \text{pecking}})$. □

C.2 | Second round of clearing with pecking order

We now adapt the second round of clearing by Ghamami et al. (2022) to the pecking order setting. Let $(\pi^{*,R1, \text{pecking}}, p^{*,R1, \text{pecking}}) \in [0, 1] \times [0, \bar{p}^{R1}]$ be the greatest fixed point of $\Phi^{R1, \text{pecking}}$.

Again, the payments outstanding at the start of the second round are given by $\bar{p}^{R2, \text{pecking}} = \bar{p}^{R1} - p^{*,R1, \text{pecking}} \in [0, \bar{p}^{R1}]$. Consider the function $\Phi^{R2, \text{pecking}} : [0, \pi^{*,R1, \text{pecking}}] \times [0, \bar{p}^{R2}] \rightarrow [0, \pi^{*,R1, \text{pecking}}] \times [0, \bar{p}^{R2}]$. Our aim is to determine a fixed point of this function, that is, we want to find $(\pi^{*,R2, \text{pecking}}, p^{*,R2, \text{pecking}})$ such that

$$(\pi^{*,R2, \text{pecking}}, p^{*,R2, \text{pecking}}) = \Phi^{R2, \text{pecking}}(\pi^{*,R2, \text{pecking}}, p^{*,R2, \text{pecking}}),$$

where $\Phi^{\text{R2, pecking}}(\pi, p)$ is defined as follows:

$$\begin{aligned} \Phi_1^{\text{R2, pecking}}(\pi, p) &= \pi^{\star, \text{R1, pecking}} \exp(-\alpha \Gamma(\pi, p)), \\ \Phi_{2,(i,j)}^{\text{R2, pecking}}(\pi, p) &= \begin{cases} \min \left\{ \bar{p}_{ij}^{\text{R2}}, \frac{\bar{p}_{ij}^{\text{R2}}}{\sum_{k=1}^N \bar{p}_{ik}^{\text{R2}}} \sum_{k=1}^N p_{ki} \right\}, & \text{if } i \in \mathcal{C}, \\ \min \left\{ \bar{p}_{ij}^{\text{R2}}, \left(\pi r_i(\pi^{\star, \text{Round 1}}, p^{\star, \text{Round 1}}) + \sum_{k=1}^N p_{ki} - \bar{W}_{ij} \right)^+ \right\}, & \text{if } i \in \mathcal{M}, \end{cases} \end{aligned} \quad (\text{C.5})$$

where

$$\bar{W}_{ij} = \sum_{k=1}^{n_C} \bar{p}_{i, n_M + k}^{\text{R2}} \mathbb{1}_{\{\Omega_{ik} < \Omega_{ij}\}}$$

are the payment obligations of member i to CCPs that come before CCP j in the pecking order.

As before, $\Gamma(\pi, p)$ denotes the total shares of collateral sold in the second round, that is,

$$\Gamma(\pi, p) = \sum_{i=1}^N \Gamma_i(\pi, p),$$

where the total shares of collateral sold by node $i \in \mathcal{N}$ is given by

$$\Gamma_i(\pi, p) = \min \left\{ r_i(\pi^{\star, \text{R1, pecking}}, p^{\star, \text{R1, pecking}}), \frac{1}{\pi} \max \left\{ 0, \sum_{j=1}^N \bar{p}_{ij}^{\text{R2, pecking}} - \sum_{j=1}^N p_{ji} \right\} \right\},$$

if $\pi > 0$. For $\pi = 0$, we set

$$\Gamma_i(\pi, p) = \begin{cases} r_i(\pi^{\star, \text{R1, pecking}}, p^{\star, \text{R1, pecking}}), & \text{if } i \in \mathcal{D}(p^{\star, \text{R1, pecking}}) \text{ and } \max \left\{ 0, \sum_{j=1}^N \bar{p}_{ij}^{\text{R2, pecking}} - \sum_{j=1}^N p_{ji} \right\} > 0, \\ 0, & \text{otherwise.} \end{cases}$$

Furthermore, $r_i(\pi^{\star, \text{R1, pecking}}, p^{\star, \text{R1, pecking}})$ is the collateral returned to node $i \in \mathcal{N}$ and is defined as

$$r_i(\pi^{\star, \text{R1, pecking}}, p^{\star, \text{R1, pecking}}) = \begin{cases} \sum_{j=1}^N (m_{ij} - \Delta_{ij}(\pi^{\star, \text{R1, pecking}}, p^{\star, \text{R1, pecking}})), & \text{if } i \in \mathcal{D}(p^{\star, \text{R1, pecking}}), \\ \sum_{j \in \mathcal{D}(p^{\star, \text{R1, pecking}})} m_{ij}, & \text{if } i \in \mathcal{N} \setminus \mathcal{D}(p^{\star, \text{R1, pecking}}). \end{cases}$$

In our setting, the market consists of clearing members and CCPs. Since we assume that CCPs do not post IMs to their clearing members, only clearing members can have collateral returned to them in Round 2. In particular, $r_i(\pi^{\star, \text{R1, pecking}}, p^{\star, \text{R1, pecking}}) = 0$ for all $i \in \mathcal{C}$.

Lemma C.3 (Properties of $\Phi^{\text{R2, pecking}}$). *Let $\Phi^{\text{R2, pecking}} : [0, \pi^{\star, \text{R1, pecking}}] \times [0, \bar{p}^{\text{R2, pecking}}] \rightarrow [0, \pi^{\star, \text{R1, pecking}}] \times [0, \bar{p}^{\text{R2, pecking}}]$ be the function defined in Equation (C.5), then $\Phi^{\text{R2, pecking}}$ is order-preserving.*

Proof of Lemma C.3. Let $\tilde{\pi}, \pi \in [0, \pi^{*,R1, pecking}]$ with $\tilde{\pi} \leq \pi$ and let $\tilde{p}, p \in [0, \bar{p}^{R2, pecking}]$ with $\tilde{p}_{ij} \leq p_{ij}$ for all $i, j \in \mathcal{N}$.

We first show that $\Phi_1^{R2, pecking}$ is order-preserving. To see that for all $i \in \mathcal{N}$, it holds that $\Gamma_i(\pi, p) \leq \Gamma_i(\tilde{\pi}, \tilde{p})$, we consider three cases.

Case 1: Let $\tilde{\pi} > 0$. Then, $0 < \tilde{\pi} \leq \pi$ and therefore

$$\begin{aligned} \Gamma_i(\pi, p) &= \min \left\{ r_i(\pi^{*,R1, pecking}, p^{*,R1, pecking}), \frac{1}{\pi} \max \left\{ 0, \sum_{j=1}^N \bar{p}_{ij}^{R2, pecking} - \sum_{j=1}^N p_{ji} \right\} \right\} \\ &\leq \min \left\{ r_i(\pi^{*,R1, pecking}, p^{*,R1, pecking}), \frac{1}{\pi} \max \left\{ 0, \sum_{j=1}^N \bar{p}_{ij}^{R2, pecking} - \sum_{j=1}^N \tilde{p}_{ji} \right\} \right\} \\ &\leq \min \left\{ r_i(\pi^{*,R1, pecking}, p^{*,R1, pecking}), \frac{1}{\tilde{\pi}} \max \left\{ 0, \sum_{j=1}^N \bar{p}_{ij}^{R2, pecking} - \sum_{j=1}^N \tilde{p}_{ji} \right\} \right\} = \Gamma_i(\tilde{\pi}, \tilde{p}). \end{aligned}$$

Case 2: Let $0 = \tilde{\pi} = \pi$, then it follows directly from the definition that $\Gamma_i(\pi, p) = \Gamma_i(\tilde{\pi}, \tilde{p})$.

Case 3: Let $0 = \tilde{\pi} < \pi$. If $i \in D(p^{*,R1, pecking})$ and $\max \left\{ 0, \sum_{j=1}^N \bar{p}_{ij}^{R2, pecking} - \sum_{j=1}^N p_{ji} \right\} > 0$, then

$$\begin{aligned} \Gamma_i(\tilde{\pi}, \tilde{p}) &= r_i(\pi^{*,R1, pecking}, p^{*,R1, pecking}) \\ &\geq \min \left\{ r_i(\pi^{*,R1, pecking}, p^{*,R1, pecking}), \frac{1}{\pi} \max \left\{ 0, \sum_{j=1}^N \bar{p}_{ij}^{R2, pecking} - \sum_{j=1}^N p_{ji} \right\} \right\} = \Gamma_i(\pi, p), \end{aligned}$$

otherwise it holds that $\Gamma_i(\tilde{\pi}, \tilde{p}) = 0 = \Gamma_i(\pi, p)$.

Hence, $\Gamma(\pi, p) = \sum_{i=1}^N \Gamma_i(\pi, p) \leq \sum_{i=1}^N \Gamma_i(\tilde{\pi}, \tilde{p}) = \Gamma(\tilde{\pi}, \tilde{p})$ and therefore

$$\Phi_1^{R2, pecking}(\pi, p) = \pi^{*,R1, pecking} \exp(-\alpha \Gamma(\pi, p)) \geq \pi^{*,R1, pecking} \exp(-\alpha \Gamma(\tilde{\pi}, \tilde{p})) = \Phi_1^{R2, pecking}(\tilde{\pi}, \tilde{p}).$$

It is clear from the definition of $\Phi_2^{R2, pecking}$ that $\Phi_{2,(i,j)}^{R2, pecking}(\tilde{\pi}, \tilde{p}) \leq \Phi_{2,(i,j)}^{R2, pecking}(\pi, p)$ for all $i, j \in \mathcal{N}$. □

Theorem C.4 (Existence of a least and greatest price-payment equilibrium in Round 2 in the setting with a pecking order). *Let $\Phi^{R2, pecking} : [0, \pi^{*,R1, pecking}] \times [0, \bar{p}^{R2, pecking}] \rightarrow [0, \pi^{*,R1, pecking}] \times [0, \bar{p}^{R2, pecking}]$ be the function defined in Equation (C.5).*

1. *The set of fixed points of $\Phi^{R2, pecking}$ is a complete lattice. In particular, $\Phi^{R2, pecking}$ admits a greatest and a least fixed point.*
2. *Let $(\pi^{(0)}, p^{(0)}) = (\pi^{*,R1, pecking}, \bar{p}^{R2})$ and define recursively for $k \in \mathbb{N}_0$*

$$(\pi^{(k+1)}, p^{(k+1)}) = \Phi^{R2, pecking}(\pi^{(k)}, p^{(k)}).$$

Then,

- (a) *$(\pi^{(k)}, p^{(k)})_{k \in \mathbb{N}_0}$ is a monotonically nonincreasing sequence, that is, $\pi^{(k+1)} \leq \pi^{(k)}$ and $p_{ij}^{(k+1)} \leq p_{ij}^{(k)}$ for all $i, j \in \mathcal{N}$ and for all $k \in \mathbb{N}_0$.*

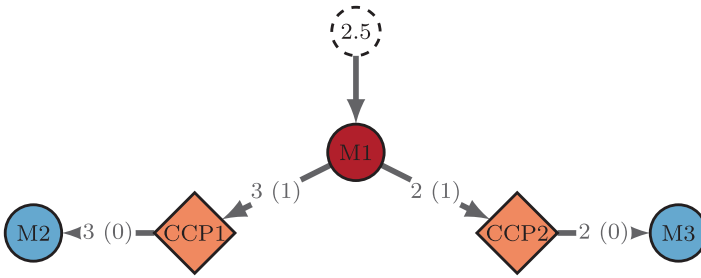


FIGURE C.1 Example in which clearing with a pecking order can reduce the number of contagious defaults. [Color figure can be viewed at wileyonlinelibrary.com]

(b) The limit $\lim_{k \rightarrow \infty} (\pi^{(k)}, p^{(k)})$ exists and is the greatest fixed point of $\Phi^{R2, \text{pecking}}$.

Proof of Theorem C.4.

1. We will prove the statement using Tarski’s fixed point theorem (Tarski, 1955). First, $[0, \pi^{*,R1, \text{pecking}}] \times [0, \bar{p}^{R2, \text{pecking}}]$ is a complete lattice with respect to the component-wise ordering. Second, it follows directly from the definition of $\Phi^{R2, \text{pecking}}$ in Equation (C.5) that indeed $\Phi^{R2, \text{pecking}} : [0, \pi^{*,R1, \text{pecking}}] \times [0, \bar{p}^{R2, \text{pecking}}] \rightarrow [0, \pi^{*,R1, \text{pecking}}] \times [0, \bar{p}^{R2, \text{pecking}}]$. Third, $\Phi^{R2, \text{pecking}}$ is an order-preserving function by Lemma C.3. Hence, by Tarski’s fixed point theorem, the set of fixed points of $\Phi^{R2, \text{pecking}}$ is a complete lattice and hence a least and greatest fixed point exist.
2. Since $\Phi^{R2, \text{pecking}}$ is right-continuous, the same arguments as in the proof of Theorem C.2 (part 2) can be used to prove the statement. □

C.3 | Pecking order: Two simple examples

We now show that clearing with a pecking order can lead to a different equilibrium compared to clearing based on the pro rata rule. We provide two examples, the first showing situations when a pecking order can reduce the number of contagious defaults, and the second illustrating that clearing with a pecking order can also increase the number of contagious defaults. We consider a similar situation as in Example 1 in Subsection 3.1, where a joint clearing member defaults.

C.3.1 | Example #1: Clearing with a pecking order can reduce the number of contagious defaults

We consider a system consisting of $n_C = 2$ CCPs and $n_M = 3$ clearing members. Figure C.1 provides an illustration of the network of payment obligations. The weights along the edges represent the payment obligation due from i to j in the first round, that is, \bar{p}_{ij}^{R1} , and the numbers in parentheses represent the corresponding IMs (m_{ij}). For simplicity, we assume that the liquidity buffers are zero for all nodes except for the joint clearing member M1, which has a liquidity buffer of 2.5.

There is one joint clearing member (M1) that clears at both CCPs. The other two clearing members only clear at one CCP each (M2 at CCP1 and M3 at CCP2). Again we label the clearing members M_i with index i for $i \in \{1, 2, 3\}$, CCP1 with index 4 and CCP2 with index 5 in the matrices

and vectors below. Formally,

$$\bar{p}^{R1} = \begin{pmatrix} 0 & 0 & 0 & 3 & 2 \\ 0 & 0 & 0 & 0 & 0 \\ 0 & 0 & 0 & 0 & 0 \\ 0 & 3 & 0 & 0 & 0 \\ 0 & 0 & 2 & 0 & 0 \end{pmatrix}, \quad m = \begin{pmatrix} 0 & 0 & 0 & 1 & 1 \\ 0 & 0 & 0 & 0 & 0 \\ 0 & 0 & 0 & 0 & 0 \\ 0 & 0 & 0 & 0 & 0 \\ 0 & 0 & 0 & 0 & 0 \end{pmatrix}, \quad b = (2.5, 0, 0, 0, 0)^T.$$

The joint clearing member M1 is the only node in fundamental default, that is, $\mathcal{F} = \{1\} = \{M1\}$. We assume that $\gamma_i^{(1)}, \gamma_i^{(2)} \in [0, 1]$ for all $i \in \mathcal{N}$ and assume that $\alpha = 0$.

Then, if we use clearing with pro rata payments, that is, by using Φ^{R1} and Φ^{R2} in Equations (1) and (2), respectively, then both CCPs default. In particular, here

$$p^{*,R1} = \begin{pmatrix} 0 & 0 & 0 & \frac{8}{3} & \frac{11}{6} \\ 0 & 0 & 0 & 0 & 0 \\ 0 & 0 & 0 & 0 & 0 \\ 0 & \frac{8}{3} & 0 & 0 & 0 \\ 0 & 0 & \frac{11}{6} & 0 & 0 \end{pmatrix},$$

and $\Delta = 2$, that is, all IMs are used in the first round. Therefore, no IMs are returned in round 2 and therefore $\Gamma = 0$ and $p^{*,R2} = 0$. The total shortfall is $S = 1$. Assuming illiquid collateral ($\alpha > 0$) increases the shortfall, but cannot lead to more defaults because all nodes with payment obligations are already in default.

If, however, clearing is done using a pecking order of the clearing members, that is, by using $\Phi^{R1, \text{pecking}}$ and $\Phi^{R2, \text{pecking}}$ in Equations (C.1) and (C.5) respectively—where clearing members rank CCPs according to the size of their payment obligations—then only CCP2 defaults. In particular, clearing member M1 ranks CCP1 on rank 1 of its pecking order and CCP2 on rank 2, because M1’s payment obligations to CCP1 are larger than those to CCP2. Then,

$$p^{*,R1, \text{pecking}} = \begin{pmatrix} 0 & 0 & 0 & 3 & 1.5 \\ 0 & 0 & 0 & 0 & 0 \\ 0 & 0 & 0 & 0 & 0 \\ 0 & 3 & 0 & 0 & 0 \\ 0 & 0 & 1.5 & 0 & 0 \end{pmatrix},$$

and $\Delta = 2$, that is, all IMs are used in the first round. Therefore, no IMs are returned in round 2 and therefore $\Gamma = 0$ and $p^{*,R2, \text{pecking}} = 0$. Then the total shortfall is the same as before ($S = 1$).

Hence, this is an example in which the pecking order causes a smaller number of contagious defaults. This is not always the case. Here, CCP1 is on rank 1 in M1’s pecking order. Hence, all available assets are used to pay CCP1 first before CCP2 is paid. In this example, this results in CCP1 being paid in full (all IMs are used), but now there is a payment shortfall of 1/2 from M1 to CCP2. With pro rata payments, this shortfall was only 1/6.

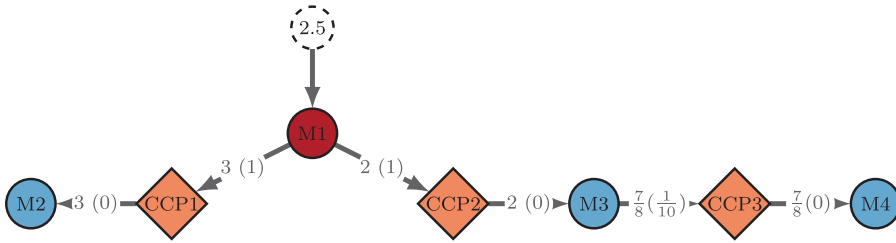


FIGURE C.2 Example in which clearing with a pecking order can increase the number of contagious defaults. [Color figure can be viewed at wileyonlinelibrary.com]

If M3 has payment obligations, the higher shortfall can cause additional contagious default, as the next example shows.

C.3.2 | Example #2: Clearing with a pecking order can increase the number of contagious defaults

For this example, we add one more CCP and one more clearing member to the previous situation. Figure C.2 provides a graphical illustration. Formally,

$$\bar{p}^{R1} = \begin{pmatrix} 0 & 0 & 0 & 0 & 3 & 2 & 0 \\ 0 & 0 & 0 & 0 & 0 & 0 & 0 \\ 0 & 0 & 0 & 0 & 0 & 0 & \frac{7}{4} \\ 0 & 0 & 0 & 0 & 0 & 0 & 0 \\ 0 & 3 & 0 & 0 & 0 & 0 & 0 \\ 0 & 0 & 2 & 0 & 0 & 0 & 0 \\ 0 & 0 & 0 & \frac{7}{4} & 0 & 0 & 0 \end{pmatrix}, \quad m = \begin{pmatrix} 0 & 0 & 0 & 0 & 1 & 1 & 0 \\ 0 & 0 & 0 & 0 & 0 & 0 & 0 \\ 0 & 0 & 0 & 0 & 0 & 0 & 0.1 \\ 0 & 0 & 0 & 0 & 0 & 0 & 0 \\ 0 & 0 & 0 & 0 & 0 & 0 & 0 \\ 0 & 0 & 0 & 0 & 0 & 0 & 0 \\ 0 & 0 & 0 & 0 & 0 & 0 & 0 \end{pmatrix}, \quad b = (2.5, 0, 0, 0, 0, 0, 0)^T.$$

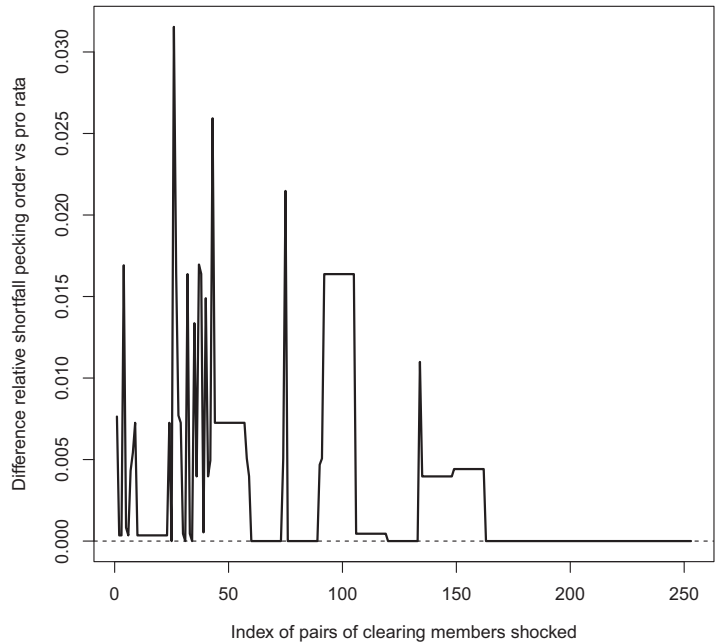
Then, if we use clearing with pro rata payments, that is, by using Φ^{R1} and Φ^{R2} in Equations (1) and (2), respectively, then as before CCP1, CCP2 are the only contagious defaults. In particular, here

$$p^{*,R1} = \begin{pmatrix} 0 & 0 & 0 & 0 & \frac{8}{3} & \frac{11}{6} & 0 \\ 0 & 0 & 0 & 0 & 0 & 0 & 0 \\ 0 & 0 & 0 & 0 & 0 & 0 & \frac{7}{4} \\ 0 & 0 & 0 & 0 & 0 & 0 & 0 \\ 0 & \frac{8}{3} & 0 & 0 & 0 & 0 & 0 \\ 0 & 0 & \frac{11}{6} & 0 & 0 & 0 & 0 \\ 0 & 0 & 0 & \frac{7}{4} & 0 & 0 & 0 \end{pmatrix},$$

and $\Delta = 2$. Furthermore, $\Gamma = 0$ and $p^{*,R2} = 0$. The total shortfall is $S = 1$.

If, however, clearing is done using a pecking order of the clearing members, that is, by using $\Phi^{R1, pecking}$ and $\Phi^{R2, pecking}$ in Equations (C.1) and (C.5), respectively, then CCP1 no longer defaults, CCP2 still defaults and now additionally both CCP3 and M3 default.

FIGURE C.3 Difference in relative shortfall when clearing members use a pecking order ($\Phi^{R1, \text{pecking}}$ and $\Phi^{R2, \text{pecking}}$) rather than the pro rata repayment (Φ^{R1} and Φ^{R2}) when different pairs of clearing members are shocked.



In particular, here

$$p^{*,R1, \text{pecking}} = \begin{pmatrix} 0 & 0 & 0 & 0 & 3 & 1.5 & 0 \\ 0 & 0 & 0 & 0 & 0 & 0 & 0 \\ 0 & 0 & 0 & 0 & 0 & 0 & 1.6 \\ 0 & 0 & 0 & 0 & 0 & 0 & 0 \\ 0 & 3 & 0 & 0 & 0 & 0 & 0 \\ 0 & 0 & 1.5 & 0 & 0 & 0 & 0 \\ 0 & 0 & 0 & 1.6 & 0 & 0 & 0 \end{pmatrix},$$

and $\Delta = 2.1$, that is, all IMs are used in the first round. Therefore, no IMs are returned in round 2 and therefore $\Gamma = 0$ and $p^{*,R2, \text{pecking}} = 0$. The total shortfall has now increased to $S = 1.3$. Hence, this is an example in which using a pecking order for clearing can increase the total shortfall.

C.4 | Pecking order: A case study

We now investigate the impact of clearing with pecking order when conducting a stress test as before using the IRS data by wiping out the liquidity buffers of different pairs of clearing members. Figure C.3 shows the difference in the shortfall between clearing with pecking order and clearing pro rata for different combinations of clearing member pairs being shocked. Here, we assume that the collateral is liquid and that there are no further frictions. We find that in this example clearing with a pecking order results in a slightly larger shortfall in the system.